Development of a Semi-active Suspension System for Lightweight Automobiles

Sheetanshu Tyagi

Thesis submitted to the faculty of the Virginia Polytechnic Institute and State University in partial fulfillment of the requirements for the degree of

Master of Science

In

Mechanical Engineering

Saied Taheri (Chair)

Mehdi Ahmadian

Corina Sandu

June 17th, 2016

Blacksburg, VA

Keywords: semi-active, damper, testing, design, suspension

Development of a Semi-active Suspension System for Lightweight Automobiles

Sheetanshu Tyagi

ABSTRACT

Vehicle suspension systems play an integral role in influencing the overall performance of a vehicle. The suspension system of a vehicle performs multiple tasks, such as maintaining contact between the tires and the road and isolating the frame of the vehicle from road-induced vibration and shocks. A significant amount of research has been directed to improving the performance of the suspension system by varying the damping coefficient so as to alter the frequency response of the system.

This study describes the development of such a damper. The goal of this research has been to design, model, fabricate and test a novel semi-active damper. The damper consists of two independent electronically controlled units placed in series with one another. The system was initially simulated using a 2 DOF quarter-car model and the performance characteristics of the damper were outlined. Following that, multiple design iterations of the damper were created and a MATLAB/Simulink model was used to simulate physical and flow characteristics of the damper. After the design and analysis was complete, the damper was fabricated and tested using a shock dyno at CenTiRe. The test results were then compared to the simulation results so as to confirm performance of the damper. Additionally, the results obtained on the dyno were then compared against that of a relative single semi-active and passive damper.

Development of a Semi-active Suspension System for Lightweight Automobiles

Sheetanshu Tyagi

GENERAL AUDIENCE ABSTRACT

Suspension in cars is responsible for maintaining adequate amount of passenger comfort and also for maintaining tire contact with the road. Suspension is one of the primary reasons cars can absorb bumps on the road while cornering at high speeds. There has been a continuous amount of research to improve the performance of suspension by changing different parts of the suspension so that passengers can experience better comfort and handling. The objective of this thesis is to design a new damper which accomplishes the same. This damper essentially consists of two electronically controlled dampers placed one on top of the other. Both dampers are actively controlled with the help of sensors and actuators so as to offer optimum performance. By using two dampers, comfort and handling of the car can be simultaneously improved, something that is essentially not possible by using dampers that are currently in the market.

The damper was designed and fabricated in CenTiRe. Multiple design iterations of the double damper were created and one of the designs was then fabricated. A computer model of the damper was also created so as to be able to simulate the performance of the damper and the results obtained from the model were compared to the results obtained from the tests.

ACKNOWLEDGEMENTS

I would like to start by thanking my advisor and mentor, Dr. Saied Taheri who gave me the opportunity to work on such a project. He has been extremely grateful and supportive and I am deeply indebted to him in so many ways. I could not have asked for an advisor better than Dr. Taheri.

No project is ever possible alone and I'd like to thank Eric Pierce. Surabhi and Tariq Abuhamdia for all the help with designing and building the damper, Omid Ghasemalizadeh for all his expertise with modeling and controls, Yashwanth Siramdasu for the simulation of the damper and Nishant Bhanot for helping me set up the entire rig. I'd also like to thank Travis Jones from Go Race, Carter from Intercomp Racing and Russell Drumheller from Mount Precision for their equipment and help with the project.

I'd also like to thank my parents for allowing me the opportunity to be here in the first place and for doing everything they have done for me and so much more. They have been extremely encouraging of my decision and none of this would have been possible without their love and guidance. I'd also like to thank Srishti Parakh for all the mental and emotional support to push me through this. Lastly, I'd like to thank Dr. Sandu and Dr. Ahmadian for all the valuable feedback and the mechanical and graduate department at Virginia Tech for their time and support.

Contents

LIST OF FIGURES

LIST OF TABLES

LIST OF SYMBOLS

Symbol	*Definition, Units*
A	Area, in^2
A_{sa}	Area of semi-active orifice valve, in^2
A_c	Area of compression chamber, in^2
A_{dyno}	Amplitude for sine wave of dyno
A_{gp}	Area of gas piston, in^2
A_o	Area of piston orifice, in^2
A_r	Area of rebound chamber, in^2
$A_{v,flow}$	Area through which valve flow occurs, in^2
A_{rod}	Area of rod, in^2
A_v	Area of valve on which pressure acts, in^2
C_d	Dynamic discharge coefficient
$C_{d,b}$	Dynamic discharge coefficient for the bleed orifice
C_f	Momentum adjustment coefficient
D_{sa}	Diameter of semi-active orifice valve, in
D_o	Diameter of piston orifice, in
D_p	Diameter of piston, in
D_v	Diameter of the valve, in
E	Modulus of elasticity, lbs/in2
F	Damping force, lbs
F_{body}	Input force from lower damper to moving body

F_{upper}	Force at upper eyelet of upper damper
F_{dyno}	Frequency of sine wave for dynamometer motion, Hz
F_{sp}	Preload force on shims, lbs
F_{upper_input}	Input force from lower damper to upper damper
F_{lower}	Damping force experienced by lower damper
k	Shim stiffness, lbs/in
l	Length of piston leakage gap, in
l_g	Length of the gas chamber, in
m_{gp}	Mass of gas piston, lb
m_p	Mass of the piston/rod assembly, lb
m_{body}	Mass of entire connecting body assembly, lb
p	Pressure, lbs/in2
p_c	Pressure in the compression chamber, lbs/in^2
p_{cu}	Pressure in the upper compression chamber, lbs/in^2
p_{cl}	Pressure in the lower compression chamber, lbs/in^2
p_i	Initial Pressure in ideal gas equation, lbs/in^2
p_r	Pressure in the rebound chamber, lbs/in^2
p_{rl}	Pressure in the lower rebound chamber, lbs/in^2
p_{ru}	Pressure in the upper rebound chamber, lbs/in^2
p_f	Final Pressure in ideal gas equation, lbs/in^2
p_g	Pressure in the gas chamber, lbs/in^2
p_{gi}	Initial pressure in the gas chamber, lbs/in^2
V_i	Initial volume of gas chamber, in^3

V_f	Final volume of gas chamber, in^3
Q	Total volumetric flow rate, in^3/sec
Q'	Equivalent flow rate due to the rod insertion, in^3/sec
Q_{sa}	Semi-active valve flow rate, in^3/sec
Q_{sal}	Semi-active valve flow rate of lower damper, in^3/sec
Q_{sau}	Semi-active valve flow rate of upper damper, in^3/sec
Q_p	Piston flow rate, in^3/sec
Q_{pl}	Piston flow rate of lower piston, in^3/sec
Q_{pu}	Piston flow rate of upper piston, in^3/sec
Q_{lp}	Piston leakage flow rate, in^3/sec
x_{dyno}	Displacement input from dyno, in
$\dot{x_{dyno}}$	Velocity input from dyno, in/sec
$\ddot{x}_{dyno}$	Acceleration input from dyno, in/sec^2
x_{body}	Displacement of connecting body, in
$\dot{x_{body}}$	Velocity of connecting body, in/sec
$\ddot{x}_{body}$	Acceleration of connecting body, in/sec^2
z	Displacement of gap piston, in
$\dot{z}$	Velocity of gap piston, in
$\ddot{z}$	Acceleration of gas piston, in/sec^2
y	Valve opening distance, in
α	Area flow correction factor
β	Fluid compressibility, ft^2/lb

β'	Effective compressibility including cylinder wall compliance, ft^2/lb
γ	Correction factor used for correlating model to experimental data
Δp_{po}	Pressure drop across the piston orifice, lbs/in^2
Δp_{valve}	Pressure drop across the valve shim, lbs/in^2
ΔV	Volume change in gas chamber, in^3
μ	Dynamic viscosity, $lbs.s/in^2$
σ	Density, lbs/in^3

Chapter 1
INTRODUCTION

Ride comfort and road handling have usually been considered the most important factors in evaluating suspension performance. Ride comfort is proportional to the absolute acceleration of the vehicle body, while road handling is linked to the relative displacement between vehicle body and the tires [1]. Most automobile suspension systems consist of a damper, a spring and a set of linkages as shown in figure 1. The three parts of the suspension system are responsible for varying the resultant absolute acceleration and relative displacement. Each of these elements has their own functional purpose within the suspension system; the spring element provides energy storage by providing stiffness, the damping element provides energy dissipation as a function of its damping coefficient, and the linkages provide mechanism constraints on the suspension motion and controls motion.

Figure 1: *Parts of a typical vehicle suspension system.*

Used under Fair Use 2016 [4]

With the advent of sophisticated electronics in the last few decades, suspension performance has drastically enhanced beyond the traditional capabilities of a passive suspension system [2]. Passive systems are limited in performance and in one way or another have to make a compromise between the two aforementioned properties. This can be modified by equipping a suspension system with sensors, controllers and control algorithms, active changes to the various properties can be made. This thesis will focus and delve deeper into the design and modeling of one such system, a semi-active double damper.

BACKGROUND

The suspension system as mentioned is a combination of various components and properties. This introduction chapter outlines the three main subject matters. It will deal with the various ways suspension systems are classified. It will then review the various advanced suspension dampers currently in use, the designs and modeling techniques used for them and end with the direct motivation for this thesis. Due to the scope of the topic, suspension geometries and performance indexes will not be looked into as they are not relevant to the contents of this thesis. The Introduction chapter is finalized with objectives and a brief outline of the thesis.

1.1 Vehicle suspension system

The primary function of the vehicle suspension system is to provide a comfortable ride, through isolation of the vehicle body from road irregularities, and enhance the ride handling by producing a continuous road-wheel contact.

According to the level of controllability, suspension systems are classified as passive, active, or semi-active as shown in figure 2. Aside from the inherent advantages and disadvantages of each type, all of them in some way utilize the spring and damper units. Suspension systems can be classified in multiple ways. The focus here will be to classify suspension systems based on method of operation.

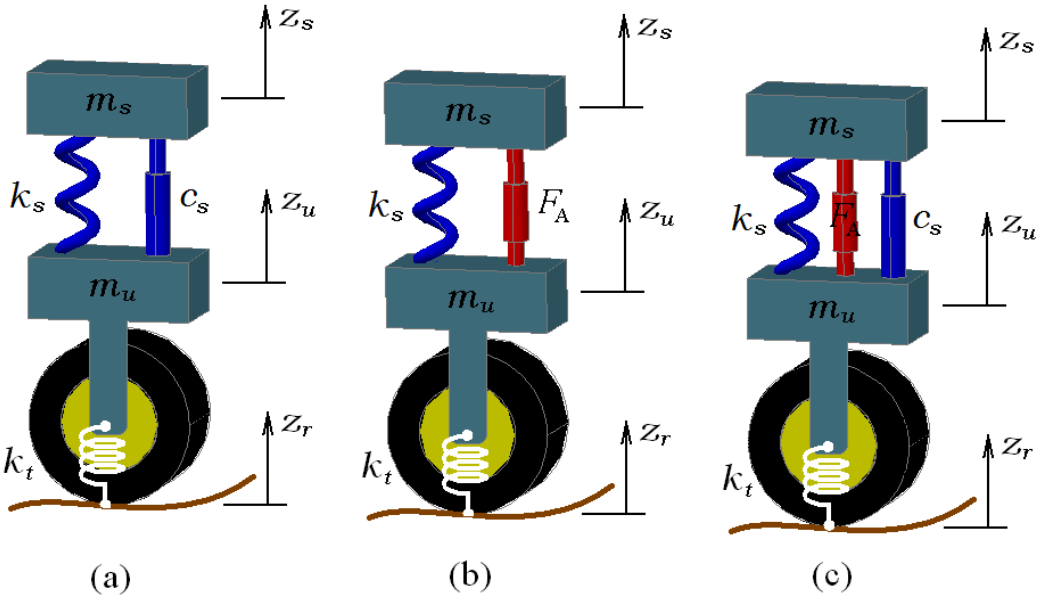

Figure 2: *2 DOF definitions for: (a) Passive (b) Semi-active (c) Active suspension. Used under Fair Use 2016* [5]

A. Passive suspension systems

Passive suspension systems comprise of all forms of conventional suspension systems that usually consist of some type of spring and damper but are completely devoid of any real time electronic control. The spring and damper used are usually designed keeping in mind a fixed spring stiffness and damping coefficient. Generally, softer dampers provide a more comfortable ride, while stiffer ones provide better stability and thus better road handling. Lately, a lot of manufacturers have tried building parametric designs where progressive springs and manually adjustable damping is used but even these suffer from the drawbacks that conventional systems have. A lot of modern dampers allow the user to have real time control by manually adjusting a lever that changes the orifice area [3]. Moreover the main concern in suspension design and control is the fact that currently, achieving improvement in these two objectives poses a challenge because these objectives always conflict with each other in some part of motion due to the very characteristic of its design, as seen in figures 3 and 4 [4]. It is impossible to accurately obtain the two conflicting objectives at a single instant of time in a passive system. But the almost ubiquitous use of passive suspension systems within most automobiles stems from their design simplicity and reliability and their low associated manufacturing cost. Thus, these factors make them attractive relative to more advanced suspension systems.

It can be seen that by changing the damping coefficient we get a change in the frequency response as frequency varies. At lower frequencies, it is preferable to have a higher damping coefficient for both the road-to-chassis frequency response and for road-to-tire deflection but this changes for higher frequencies where it is

preferred to have lower damping for higher frequencies for the road-to-chassis frequency response. This conflicting response is the primary reason why passive suspension systems are not desirable.

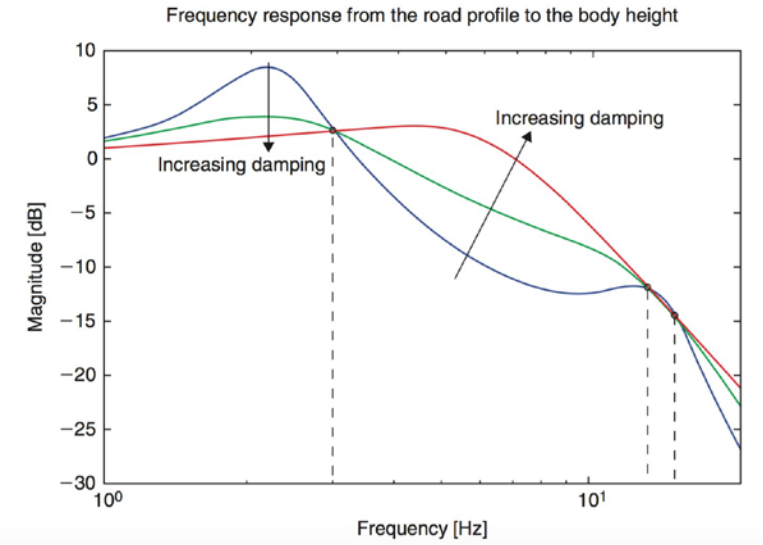

***Figure 3**: Example of a road-to-chassis frequency response. Used under Fair Use 2016 [4]*

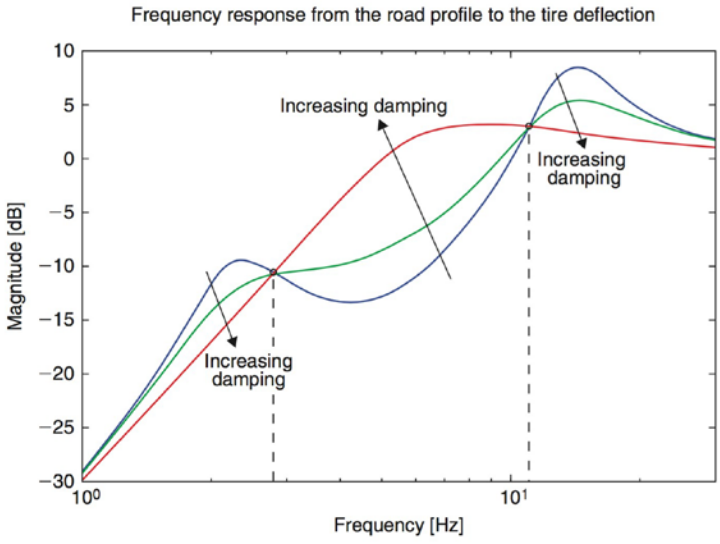

***Figure 4**: Example of a road-to-tire frequency response. Used under Fair Use 2016 [4]*

B. Semi-active suspension systems

Semi-active suspension systems are electro mechanical control devices with the capability to vary the amount of energy dampers dissipate using a small source of power. Semi-active suspension systems are essentially passive systems in which the damping and stiffness properties are allowed real time variation to suit current demand. Varying the input voltage or current to a semi-active damper creates change in performance. They are a compromise between the active and passive systems and allow a variation in the stiffness or damping properties of the system but do not require any force input into the system [5].

According to variation in stiffness and damping, there are five main classes of electronically controlled suspensions as shown in Figure 5 [6]:

- Load-leveling suspension, which is an active suspension system with an actuation bandwidth well below the main suspension dynamics.
- Slow-active suspensions that is an active suspension system with a bandwidth in between body and wheel dynamics.
- Adaptive suspensions which have a slowly modified damping ratio; typically this modification is simply made with an open-loop architecture.
- Semi-active suspensions which have a damping ratio modified in a closed-loop configuration over a large bandwidth.

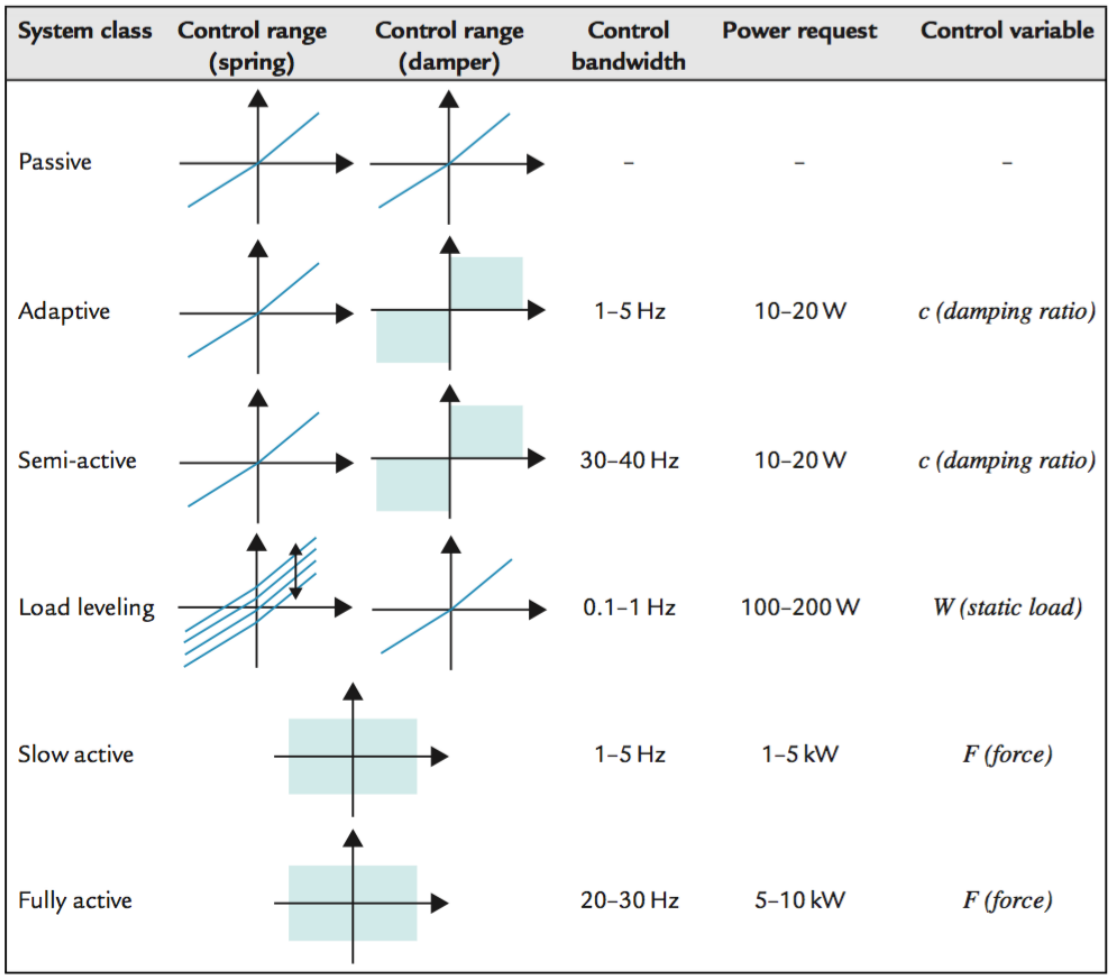

***Figure 5**: List of electronically controlled suspension systems.*

Used under Fair Use 2016 [4]

Most commercially available semi-active suspension systems are constituted of load leveling systems (e.g. gas springs) and semi-active dampers as the performance to cost ratio of these units is relatively high. In all cases, modulating the damping properties requires a small power source, but does not introduce energy into the suspension system [7]. Compared to passive suspension systems, their designs are more complex, they have reduced reliability, and are relatively more expensive to manufacture. Overall however, the impact of semi-active suspension systems on vehicle dynamics performance surpasses the performance that passive suspension

systems can achieve and has been used on modern luxury automobiles as they extend the possible range of damping and springing characteristics obtainable from a passive system. Multiple designs and arrangements of these dampers exist and those will be looked into with greater detail later.

C. Active suspension systems

Active suspension refers to a system that uses an active power source to actuate the suspension links by constantly changing the output force in real time [3].

In an active suspension, controlled forces are introduced to the suspension by means of hydraulic or electric actuators, between the sprung and unsprung-mass of the wheel assemblies. Many researchers have studied the effect of adding an active damping force to the suspension system in the past [8] [9]. An active suspension system measures the input being obtained from the road profile, and applies a reactive force as a response. A variable force is provided by the active suspension at each wheel to continuously modify the ride and handling characteristics. The key difference between semi-active and active suspension systems is that the latter applies an external force to the vehicle body either in an upward or downward direction, regardless of the absolute vehicle body velocity. Active suspension overcomes the compromises required in tuning passive systems.

Although active suspensions have superb performance, the practical implementation of active suspension in vehicles has been limited due to their high weight, cost, power consumption, and reduced reliability that are not justified by the limited incremental benefit to the passenger [10]. Moreover the performance gap between semi-active and active systems does not compensate for the drastic increase in cost. The Bose active suspension system as shown in figure 6 is one of

the only commercially available active suspension system.

Figure 6: *Bose active suspension system. Used under Fair Use 2016* [4]

1.2 Types of semi-active suspension

As mentioned, semi-active suspension systems are composed of adjustable dampers or springs or both. A large amount of work has gone into using advanced semi-active dampers as that has a more profound impact on the two evaluation parameters, road holding and comfort. Over the years many different designs and systems have been used as semi-active dampers. This section describes some of the design techniques used to achieve adjustable damping:

- **Position controlled valves**: These mainly consist of using an electronically controlled unit like a solenoid or servo valve. These devices employ actively adjustable valves that change the orifice area through which fluid passes. The

variation in area is achieved by providing power to the electronic valve unit. This controlled application of power then allows the adjustment of the orifice area through which fluid flows. The variation in orifice area allows a change in damping coefficient that thus changes the resistive force being exerted on the damper. It can provide high speed, accurate flow control at a high operating pressure [5].

Solenoid and servo valves are ideal for this application. Servo-valves can provide very high speeds, linearity, and accuracy of flow control at high operating pressures and have been used successfully in multiple semi-active and active suspensions which use a hydraulic pump, reservoir, accumulators, etc. and hydraulic cylinders connecting the wheels to the chassis. But, servo-valves are very expensive and complicated devices. A typical servo-valve costs US$4200 [9].

Solenoid valves are used as an alternative to servo-valves and do not have as fast or accurate a response as a servo-valve; however, a servo-valve is much more expensive than a solenoid valve. A solenoid valve is much simpler in design than a servo-valve, and it could possibly be manufactured in-house, bringing the added benefit of being able to optimize the valve design for the particular application including force, stroke, and general packaging. [10] Solenoid valves have also been used in two- or three-state dampers that can change characteristics between hard damping and soft damping by opening or closing a bypass valve. These dampers have resulted in improvements in ride quality when appropriate control schemes are used. Although these dampers do not have the capability of being continuously variable, continuously variable solenoid valve dampers are also available [13]. Solenoid valves of this type have

been tested, with promising results [11].

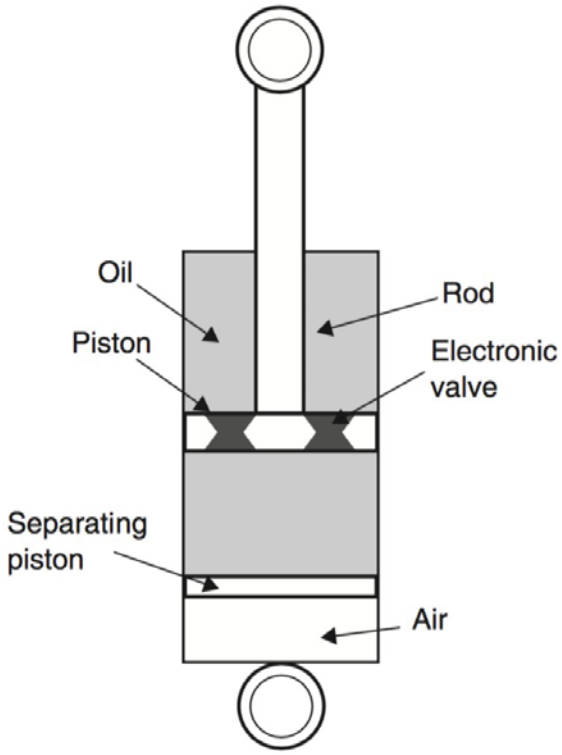

***Figure 7**: Schematic of electrohydraulic damper. Used under Fair Use 2016 [4]*

- **Electro-rheological (ER) fluid:** Electro-rheological fluids are fluids that change viscosity under the application of electric fields and therefore can be used to vary the damping force being exerted. The ER damper can be regarded as an "electric capacitor"; the external body is an anode and the piston is a cathode. The electric field appears in the space between the piston and the body. In order to obtain the necessary forces, the surface of the piston is relatively large [1]. The side effect is a minimum damping level usually greater than the minimum damping level provided by the MR damper. On the other hand, the friction effect is less harmful and the ER fluid seems to be less aggressive. But

they require very high voltages, 1-5 kV and have a very narrow working temperature range. ER fluids are also extremely expensive and difficult to use and are therefore not used commercially as extensively [12]. Moreover, at temperatures of approximately $50^{O}C$, ER activity decreases significantly and thus the temperature instability limits the potential use of the ER fluids [16].

- **Magneto-rheological (MR) fluid:** MR fluid is a non-Newtonian fluid that changes its properties in the presence of a magnetic field. Micron- size iron particles suspended in a carrier fluid (water, petroleum-based oil, or silicon-based oil) align in chain-like structures along the flux lines of a magnetic field, changing the rheological properties of the fluid. This causes the fluid to apply varying levels of resistive force to the system that thus allows change in the damping coefficient. Multiple dampers have been built and have been tested with favorable results [14] [15]. These devices use an electromagnetic coil in close proximity to the magnetorheological fluid flow to create a damping force that is adjustable by the current applied to the coil to a magnetic field. The MR fluid behaves as a liquid when no field is applied and the shock behaves like a passive shock absorber. But in the case of a magnetic field applied to the fluid, the particles form chains and the fluid becomes very viscous. This resistivity is invariably responsible for creating a certain damping force that can be varied by changing the input voltage applied. But MR dampers have been slow to commercialization because of certain inherent issues. Using MR fluids in large-scale applications requires a large amount of MR fluid which makes the device extremely heavy and expensive. Moreover MR fluids suffer from various long-term limitations such as particle settling, field saturation, wall effects, and response time which limit the prolonged use of MR suspension without issues creeping in. Even though the

response time of an MR damper is extremely fast, but MR dampers really have two time constants, t_1 is called chain formation time, which is within one milli-second. t_2 is system response, including field set up which is around 10 milli-seconds [16] [17].

Figure 8: *Examples of semi-active damper, (a) Solenoid operated electrohydraulic damper (Sachs). (b) Magnetorheological damper (Delphi). (c) Electrorheological damper (Fluidicon). Used under Fair Use 2016* [4]

The response time of using an internal and external solenoid valve are very similar to each other and are slightly higher than that of a magnetorheological fluid based damper [1]. But the cost of using an MR based damper is much higher and therefore a solenoid-based damper was chosen for the scope of this thesis.

1.3 Damper modeling

Modern dampers exhibit a response that changes the force in a proportional manner to the relative velocity. This is because damper manufacturers chose this as the

desired output result [18]. In a commercial hydraulic damper, the damping effect is caused by the fluid that passes through a complex series of orifices and valves and is therefore complex due to the number of parameters involved in the process. The force v/s velocity and force v/s displacement curves are usually recorded to gain a better understanding of the damper characteristics. The graph is used to study the behavior of the damper in compression and rebound.

Multiple models were studied and analyzed and a review was conducted to obtain a better understanding of how individual internal components and internal flows had been characterized in the past by studying the development of parametric and analytical models for damper characterization. Conventional damper models that are created by breaking down the physics of the individual components of the damper and understanding the fluid flow through each were studied. This approach has yielded good results and over the years and the standard model that was first created by Lang has been modified to obtain higher accuracy [19]. Simpler models use equations to define fluid flow without taking hysteresis into account which gives acceptable results without including the change in compression and rebound [20]. Non-linear parametric models which take into account flow restriction forces, port restriction and spring stiffness correction factors were also studied. Parameters that have to be found by using experimental results have to be recorded to be able to use this model. The main focus in this research is to focus on parametric physics based models, as they are relatively easy to implement and give a sufficiently accurate response.

1.4 Design of dampers in vehicle suspension system

Automotive dampers primarily isolate the vehicle chassis from unwanted vibrations due to the road disturbances, and provide good road handling by dissipating the energy through a series of valves or orifices. In the following subsections, different commercial damper technologies such as passive (hydraulic) and semi-active are analyzed to gain a better understanding of the design of individual components and the suspension system as a whole.

A. Passive hydraulic components

Most conventional vehicle suspension systems utilize passive dampers to provide damping. Conventional hydraulic shock absorbers suppress vehicle frame vibration by forcing oil through a piston. Holes in the piston are covered by valves, which resist the flow of the oil through the holes in a controlled manner to produce the damping effect.

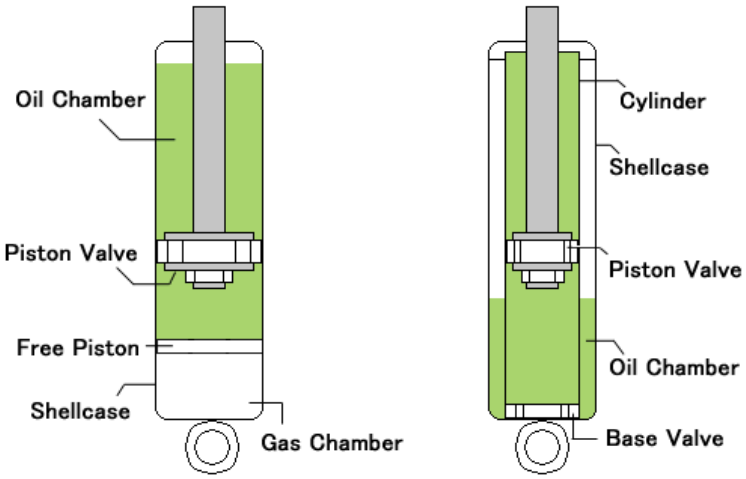

Figure 9: *Schematic of: (a) Mono tube damper. (b) Twin tube damper. Used under Fair Use 2016* [2]

Most manufacturers use multiple valves to produce this effect and also to make the compression and rebound strokes independent of each other. Based on the arrangement of the various components, there are basically two categories of passive dampers as shown in Figure 9, mono-tube and twin-tube. Unlike the twin-tube damper, a mono-tube damper is composed of one cylinder filled with oil through which a piston with an orifice is moving. Passing the fluid through the orifice causes a resultant damping force due to the pressure drop between the compression and extension chambers. The presence of the gas chamber allows the volume of the piston rod to enter the damper. The gas also adds a spring effect to the force generated by the damper, maintaining the damper at its extended length when no force is applied. The various parts that constitute a mono tube damper are shown in Figure 10 [3]. Twin-tube designs consist of an inner chamber with a piston moving in it, and the outer chamber that contains the gas chamber and acts as a reservoir for the oil. The outer chamber equalizes the oil volume changes caused by the piston rod movement. There are also two valves used in the twin-tube design: a piston valve and a foot valve.

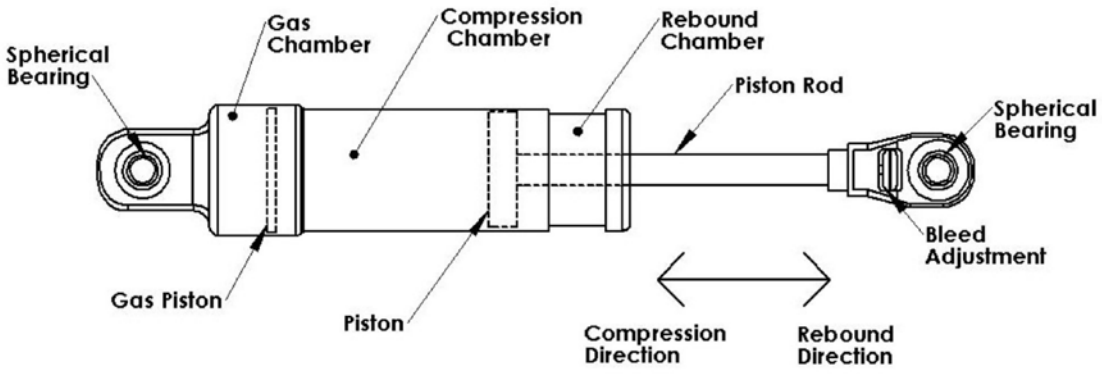

Figure 10: *Parts of a monotube damper. Used under Fair Use 2016 [6].*

Mono-tube dampers are simpler in terms of manufacturing, lighter due to the fewer parts, require higher gas pressure which leads less aeration, and are more susceptible to damage of the cylinder compared to their twin-tube counterparts. But mono tube dampers create more stable damping forces because of the larger oil capacity and improved heat dissipation In contrast; twin-tube dampers can operate with lower gas pressure, and require a shorter stroke. Twin tube dampers are also more forgiving to any external damage and also allow superior manufacturing proves which thus keep production costs low. But twin tube dampers are more complex, and have issues with dissipating the generated heat. Moreover, twin tubes don't have a separate piston for the gas reservoir that leads to unstable damping. Manufacturing twin tubes is more expensive for lower volumes and requires high levels of precision [18].

B. Semi-active components

Variable dampers vary the damping rate by varying the size of the valve opening by means of a servo-valve, shim-valving, piezoelectric actuators, solenoid-valve, or using MR-fluid in which the viscosity of the oil is varied, instead of the size of the valve opening.

Multiple patents and papers were looked into to understand more about different controllable valves and systems used. Most commercial semi-active dampers mainly use two types of controllable valves:

- **Rotating discs:** This approach mainly uses servo or stepper motors mounted either internally or externally. The motor is usually connected to a plate with

holes in it and rotates relative to another plate with holes. As the two plates move against each other, certain holes get covered and uncovered. This leads to a variable amount of fluid flowing through the piston and thus leads to variable damping [22] [23].

- **Solenoid assembly:** Most commercial electro-hydraulic dampers have chosen to use fast acting solenoid valves. Different inventors have implemented solenoid valve assemblies in multiple ways. Some use an externally mounted bi directional solenoid valve that is energized by the application of voltage. A twin tube design is used for the damper and the valve is mounted externally against the outer tube of the damper. A custom solenoid rod rests against a surface that is mounted against spring-loaded shims. On application of voltage, the solenoid moves upwards against the spring and thus allows fluid to flow through [24] [26]. Some dampers use the valve assembly such that the fluid after moving past the solenoid passes through multiple constricted passages so as to offer additional damping [25]. Examples of both cases are shown in Figure 11 [22] [26].

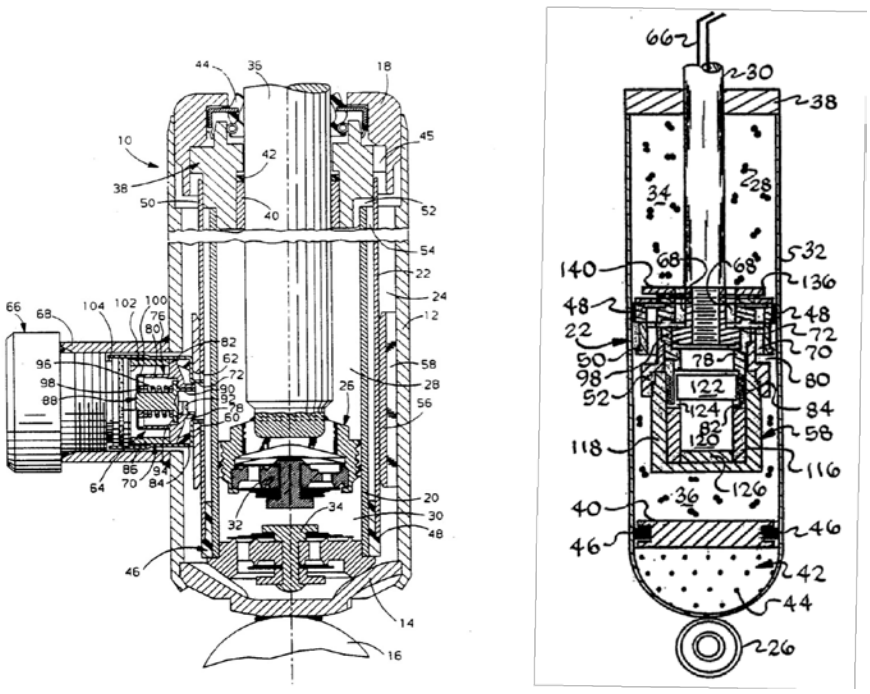

Figure 11: *Examples of types of electrohydraulic dampers: (a) Externally operated solenoid valve. (b) Internally operated motor controlled valve. Used under Fair Use 2016* [9].

1.5 Motivation

The initial motivation for this thesis was based on an idea of testing the possibility of using multiple springs and dampers to see the resultant performance of the system. In June 2014, Yashwant et al. [27] implemented a 2 DOF quarter-car model to simulate the response of a passive, semi-active and active suspension system. The semi-active damper being used in the study was comprised of two variable dampers placed in series. A combination of skyhook and ground-hook model was used as a reference in this research. The skyhook model was considered as the optimal control policy for vibration control of 1 DOF mass-spring-damper system with base excitation and the ground-hook model was considered as the optimal

control policy for the control of wheel hopping to increase the road holding capability [4]. The 2 DOF model developed for the double damper is as shown.

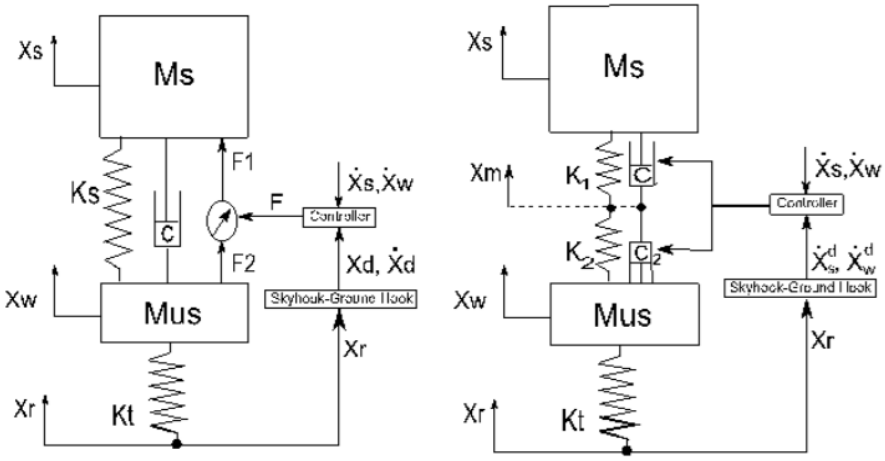

Figure 12: *2 DOF Systems: (a) Single semi-active (b) Double Semi-active*

A Lyapunov based adaptive control algorithm was developed and used for both, active and semi-active damper control. The algorithm consists of a proportional feedback part and a full dynamics feed forward part that estimates unknown model parameters online. The advantage of this method is due to its computational simplicity just like PID, and use of only a velocity sensor for each mass, thus reducing cost and computational power. From the formulations of control algorithm, the computed control forces were applied to the equations of motion of single damper and double damper *(1)* quarter-car models [4].

$$I\begin{bmatrix}\dot{X}_1\\ \dot{X}_2\\ \dot{X}_3\\ \dot{X}_4\end{bmatrix}+\begin{bmatrix}0 & -1 & 0 & 0\\ K_1/M_s & C_1/M_s & 0 & 0\\ 0 & 0 & 0 & -1\\ 0 & 0 & \frac{K_1+K_2}{M_{us}} & C_2/M_{us}\end{bmatrix}\begin{bmatrix}X_1\\ X_2\\ X_3\\ X_4\end{bmatrix}+\begin{bmatrix}0\\ A\\ 0\\ B-\frac{K_t X_R}{M_{us}}\end{bmatrix}=F \qquad (1)$$

The three damper models developed were then excited by an input road profile as shown in Figure 13. The properties of the vehicle were based on a Volkswagen Jetta and a simulation for 30 km/hr and 90 km/hr was performed.

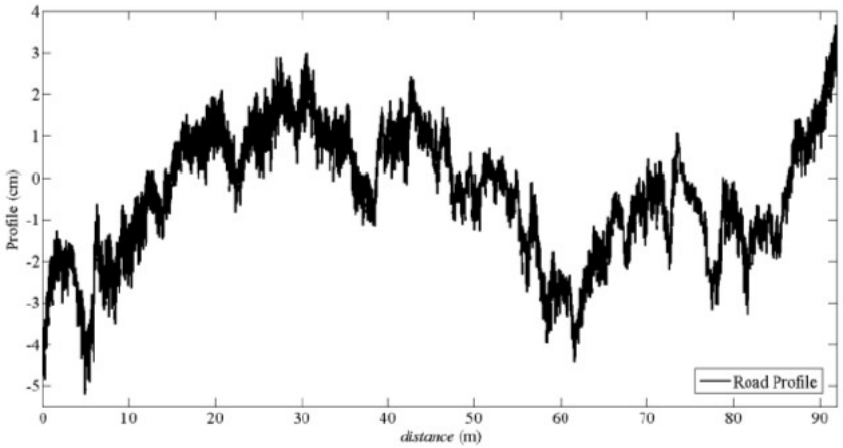

Figure 13: *Road profile used for simulation*

The simulation results (figures 14 and 15) showed that the semi-active based double damper suspension can be a substitute for active suspension. No abnormalities in suspension deflection and tire deflection from normal suspension are observed. Semi-active suspension results are constrained in saturation and energy limitation of the damper. This approach of ride control based on double damper has shown to significantly improve the ride performance of the vehicle at the reduced power consumption, cost, and complexity with more reliability.

Based on these results, it was decided to build a physical system that could act like a double damper and evaluate its properties against that of a passive, semi-active and active damper.

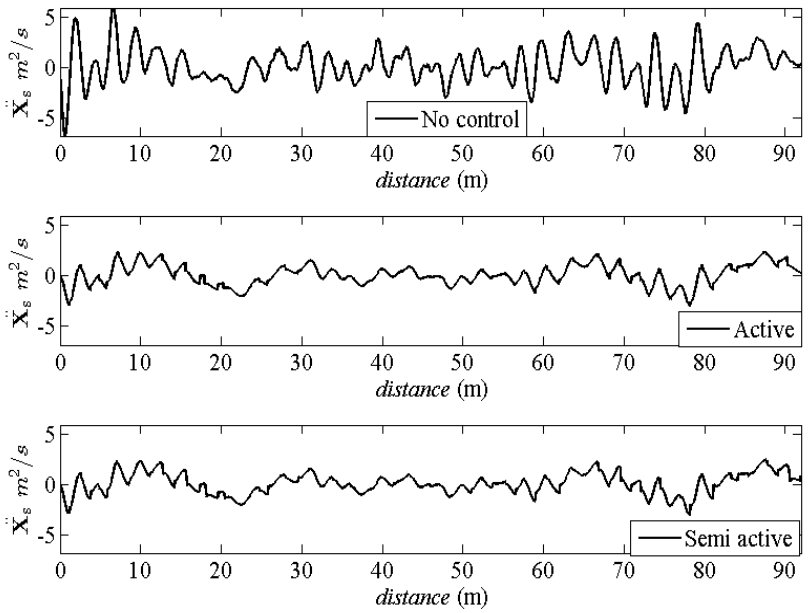

Figure 14: *Acceleration of Sprung mass at 90 Km/hr with no control, active and semi-active control.*

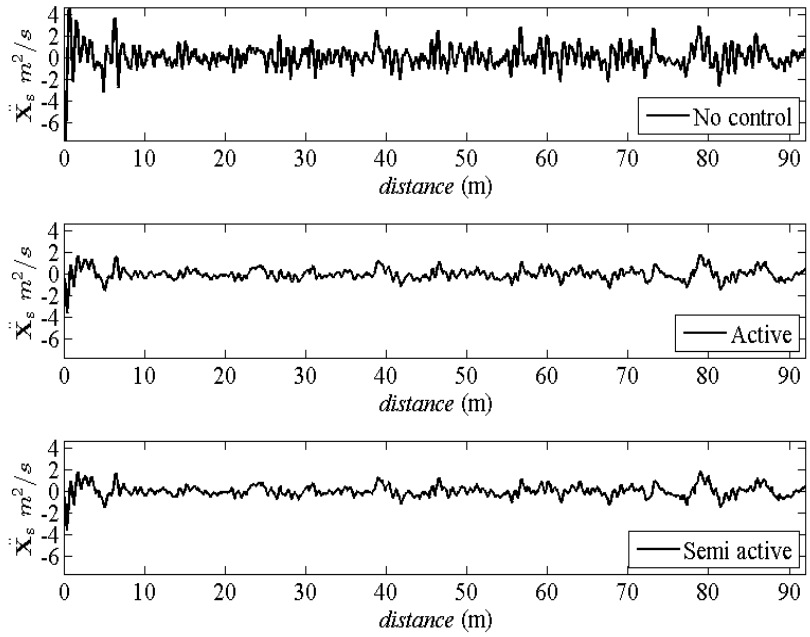

Figure 15: *Acceleration of Sprung mass at 30 Km/hr with no control, active and semi-active control*

1.6 Objectives of thesis

The simulation of the double damper initiated a study into the performance characteristics of such a semi-active system. Therefore for the scope of this thesis, it was decided to achieve the following:

1. Design and build a basic prototype of a semi active double damper.
2. Test the double damper on shock dyno to see difference in performance when compared to a single passive damper.
3. Understand fluid flow and force response by building a mathematical model to predict results obtained using a shock dyno.
4. Observe differences obtained and suggest changes to design of damper to attain better performance.

1.7 Thesis outline

This thesis focuses on the design, modeling, and dynamometer testing study of a novel semi-active suspension system. It includes the design and fabrication of the damper that is followed by modeling the flow through the damper and then validating that by real world testing on a dynamometer. This process is presented and organized in six chapters, as follows:

Chapter 1 presents a brief introduction on the vehicle suspension system, including different vehicle suspension types. That is followed with an overview of dampers in vehicle suspension, including a review of the literature on passive and semi-active dampers. This chapter concludes with a concise summary of damper

modeling and also outlines patents that were used as reference for the design of the semi-active damper.

Chapter 2 goes in to the design of the damper and outlines the various parts that were designed for the damper. The various iterations of the design have been shown. The designs of both, the single and double damper are shown and reasons for component selection are mentioned.

Chapter 3 presents the parametric model of the damper and outlines the physics that have been used to model the damper. Models for the single and double damper have been shown and equations that have been used to study the damper have been laid out.

Chapter 4 highlights the test setup and the equipment being used for testing the damper. The basis for testing the damper is outlined and the tests that are to be performed are mentioned in detail

Chapter 5 discusses the results obtained during testing of the dampers. The results are then correlated to the results obtained from the model. The results are analyzed and the physics behind the working of the damper is discussed.

Chapter 6 is the conclusion and ends with recommendations for future work to be done.

Chapter 2

Design of system

According to the results obtained from the simulation, the sprung mass acceleration and tire deflection due to the double damper were very similar to the results obtained for the active suspension. It was therefore decided to build a double damper so as to test it for real world conditions.

2.1 Design of damper

Based on the simulation performed, there were certain requirements the damper had to meet:

- Two controllable dampers had to be placed in series.
- The reference coefficients for the dampers would be obtained from the skyhook and ground-hook policy.
- Coefficients of damping had to lie within 0 and 5000 N/m/s for the roadside damper and 0 and 1500 N/m/s for the chassis side damper.

To be able to test the damper against a passive and equivalent semi-active and active damper, a testing procedure was formulated. The plan to go about designing and testing the damper was finalized as follows:

1. Pick test vehicle and finalize damper stroke and size based on stock damper characteristics.
2. Test passive damper at multiple speeds and establish benchmark damper

characteristics.

3. Design damper and implement semi-active controller.
4. Model flow through semi-active damper to be able to evaluate damper characteristics empirically.
5. Test damper on shock dynamometer and validate results obtained against results of model. Tune damper such that it matches flow in passive damper.
6. Test passive and semi-active dampers on quarter-car and compare evaluation parameters against each other.

The final objective as mentioned was to be able to test a commercially available semi-active damper (Delphi Magneride), an active damper, a passive damper and the double damper against each other to see the differences in performance. The comparison would be based on evaluating the sprung mass acceleration, unsprung mass acceleration and relative displacement so as to be able to quantify road holding and comfort [4]. The tests will be carried out on a quarter-car and then evaluated by testing on an actual test vehicle too.

It was decided to pick a particular test vehicle and decide the damper properties accordingly. A 2008 Chevrolet Silverado pickup truck was picked as the test bed and the rear damper of the vehicle was picked as our target. The quarter-car in CenTiRe is specifically designed to accommodate this suspension with ease and therefore this vehicle was picked. A Fox 2.0 mono-tube shock was picked as the benchmark shock. This shock was then tested on a dynamometer to get an idea of what the force v/s velocity and force v/s displacement curves would look like. The damper was tested for a stroke of 2” and a range of velocities from 2 in/sec up to 15 in/sec. The results of the tests at 2 in/sec are as shown.

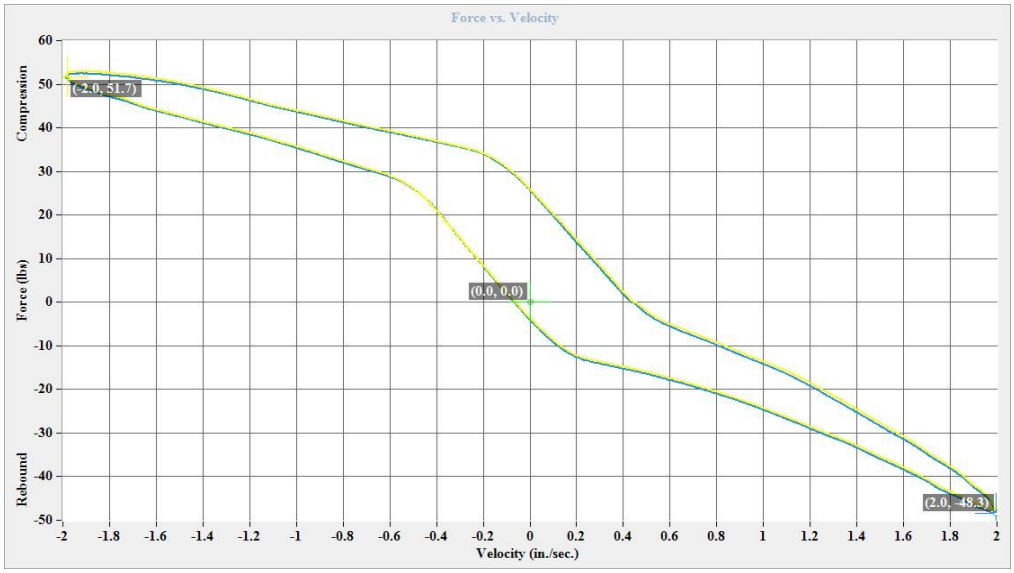

***Figure 16**: Force v/s velocity curve for FOX 2.0 Shock at 2 in/sec velocity and 2" stroke*

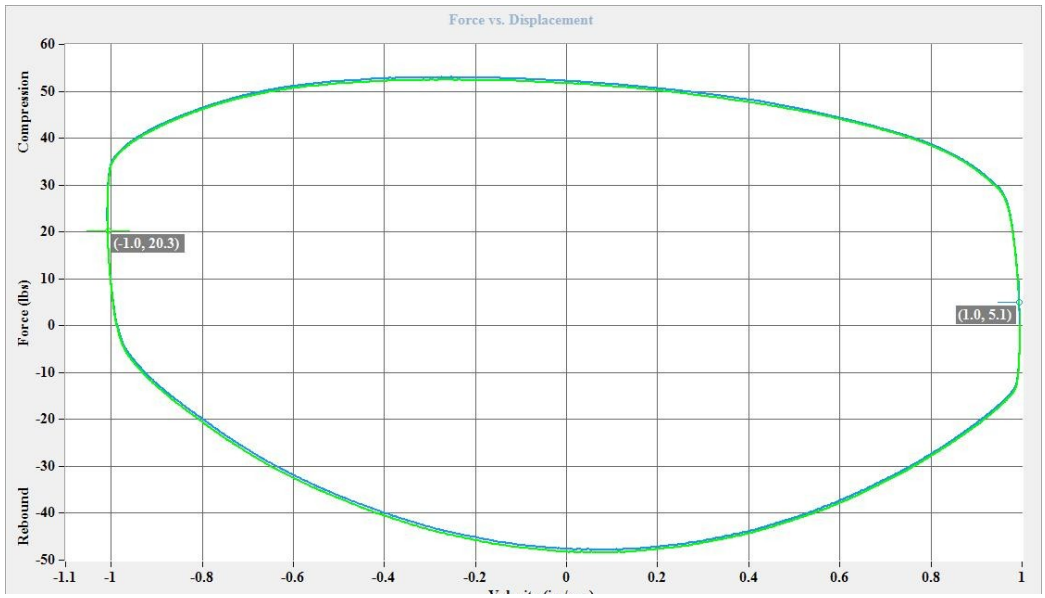

***Figure 17**: Force v/s displacement curve for FOX 2.0 Shock at 2 in/sec velocity and 2" stroke*

Once a benchmark of the tests was established, it was decided to design a single semi-active damper and a double semi-active damper so as to be able to validate the damping coefficient of the shock and see change in flow of fluid based on change in voltage. Multiple design decisions had to be made to be able to decide how the damper should function. The main characteristics of the damper that had to be finalized were:

A. Semi-active technique: MR, ER, electrohydraulic, etc.
B. Type of damper: Mono tube, twin tube, etc.
C. Semi-active mechanism: Rotary, solenoid
D. Design of individual parts and assemblies
E. Damper construction and operation

Since the damper being fabricated was supposed to be a prototype to prove a working concept, the priorities in terms of design decisions was placed on overall cost, flexibility of control and functionality. The damper was to be tested to prove a working hypothesis that two controllable dampers placed in series could function equivalent to an active damper. The focus was to be able to design and fabricate a damper that would meet the requirements of the simulation but would require limited amount of resources.

Therefore for each characteristic mentioned above, a rigorous analysis was performed to evaluate the most optimum design to be used.

A. Semi-active technique

The semi-active properties of a damper can be achieved in many ways. The most common techniques to perform the same is to use MR fluid along with a magnetic

field, or to use an electrohydraulic valve. As shown, MR fluid has been used in many dampers with favorable results but has serious limitations as mentioned earlier and is also very expensive to build from scratch. Moreover since this was to be used for a prototype damper, multiple iterations could be required. The body and magnetic field inducer also required extremely intricate design and therefore it was decided that the cost and design of the MR system would be prohibitive. An alternative electro hydraulic unit that could provide comparative performance and similar time response was to be used.

B. Type of damper

Twin tube dampers are more common for commercial applications because of the shorter stroke and easier high volume manufacturing. But twin tubes are difficult and more expensive to fabricate for lower amount of units. Using a mono tube damper allows better control of the gas pressure and fluid flow as there is only one flow path through the internal piston. Moreover the controllable valve can be placed internally or externally as a bypass. This also allows more predictive modeling of the fluid flow through the damper and allows more accurate comparison of the model against the test data. Therefore a mono-tube damper was used.

C. Semi-active mechanism

Using a controllable semi-active valve in conjunction with the internal piston can be achieved in two ways:

- Internal mechanism: This can be achieved by using a stepper motor or solenoid that controls fluid flow between the compression and rebound sides of the

piston. The difficulty in this case is to reliably use a valve submerged in fluid. This also limits the amount of damping that can be created as the unit has to be packaged in a finite amount of space.

- External by pass mechanism: This works in parallel with the internal piston and allows semi-active control of the external valve while simultaneously allowing fluid flow through the internal piston. This technique enables quicker maintenance and service of the system. This also allows to specifically measure the input and output flow rate and pressure of the bypass line.

Both approaches were investigated and a design for each was created.

The semi-active mechanism consisted of two plates with orifices in them with a plate controlled by the motor sandwiched between the two. The motor controlled the middle plate and the rotary action caused the orifice area to change. Dual action could be obtained as the fluid went through two orifices. The stock piston from the FOX shock was used to have an estimate of the area of the orifice. This assembly was designed such that the valve would be located externally as a bypass circuit. This ensures flexibility in terms of adjustment and also enables flow separation between the internal piston and external semi-active valve.

The internal mechanism used a similar rotary mechanism but was attached to the piston rod differently. The internal piston in this case did not have shims but was completely controllable. Size and packaging was a major issue when developing an internal flow semi-active valve assembly and only motors that could withstand high pressures and contact with mineral oil could be used. Also an internal piston rod that would have to have a through hole for the input wires would have to be used. This added unwanted complication to the design and therefore the external

mechanism was chosen.

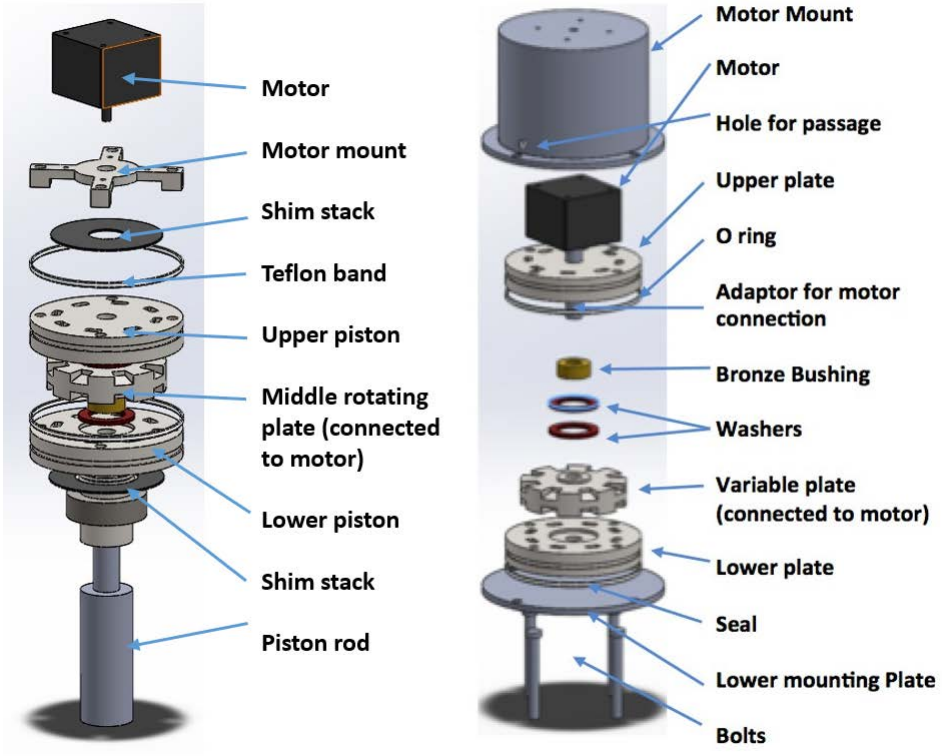

Figure 18: *Semi-active piston assembly options that were considered: (a) Internal motor controlled semi-active valve (b) External by pass motor controlled valve*

D. Design of individual parts and assemblies

Since a standard internal piston and a bypass circuit were being used, it was decided to use a stock configuration for the internal piston of the shocks. Therefore the piston rod and internal piston being used were that of a stock FOX 2.0 Shock absorber.

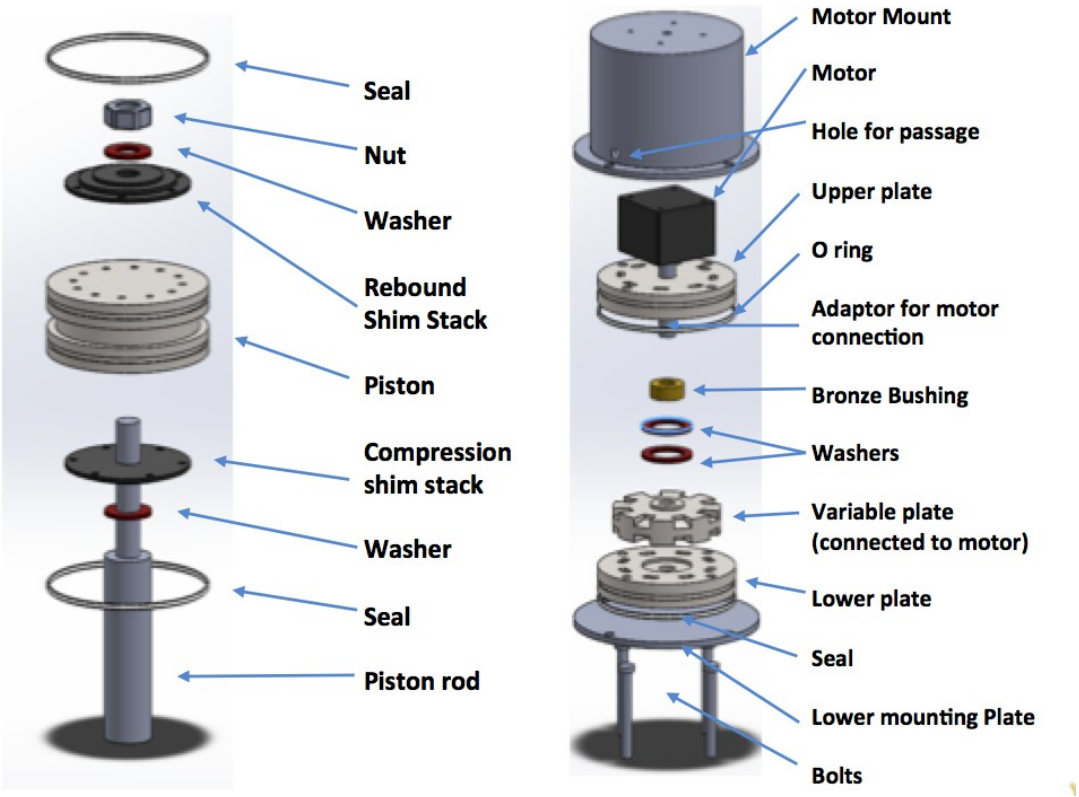

Figure 19: *Valves used for the final design: (a) Internal fixed flow piston (b) External semi-active piston*

Simplified designs of the internal piston were also created [28] so that the area of the piston could later be modified to obtain more precise control of the damping due to the internal assembly. Unlike the stock piston, a flat symmetric layout was chosen so as to ease fabrication. Shims with asymmetric holes machined on either side were used so as to obtain variable damping in rebound and compression. Multiple tests would need to be performed to estimate the relative stiffness of the semi-active valve and the internal valve to be used. That would help determine how many shims would have to be used on either side. The area of the holes used was determined based on a stock Fox 2.0 piston for an equivalent sized shock. A CAD model for the piston was created and the effective area was calculated. This was then also

replicated to create an equivalent area for the piston.

Additionally, to understand the effect of using the standard piston and rod, a solid piston was also fabricated. The solid piston was built out of a round billet of aluminum with no valving or shim stack. A 0.5 mm fixed bleed orifice was provided in the piston that ensured a safety mechanism in the case where the semi-active valve failed. This design thus results in variable fluid flow through the semi-active valve and a fixed fluid flow through the bleed orifice. This was done so as to obtain full control of the fluid flow through the semi-active valve and to check resulting fluid flow. Moreover by using this, the fluid flow can be compared to a scenario where both valves are used. The internal pistons and bearing caps were fabricated from 6061- T6 Aluminum and Nitrile rubber seals were used. Calculations and dimension analysis was performed to determine the appropriate dimensions of the seals so as to ensure perfect sealing and operation of the damper.

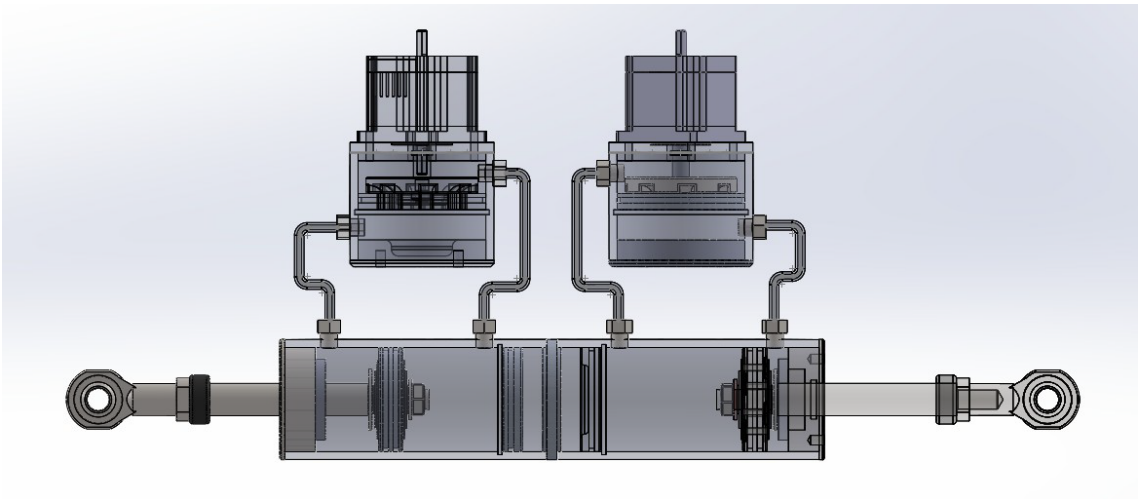

Figure 20: *Double damper with internal fixed flow pistons and external motor controlled valves*

The unit being designed was a prototype damper. So it was also decided to try using an equivalent off the shelf valve if the setup that could be purchased would be economical and would suit the purpose. Moreover since the system was not being tested on a quarter-car, any valve that created an area restriction would suit the purpose. Therefore, the HydraForce SP10-24 was used. This is a proportional solenoid-operated, 2-way, spool-type, normally closed, direct acting, screw-in hydraulic cartridge valve that provides bi-directional metering of fluid. The valve can withstand pressures up to 3000 psi and allows fluid volumes of up to 0.5 liters/sec. When energized, the SP10-24 acts as a bi-directional metering valve and allows change in area based on variation of voltage/current up to 5 V/1.2 A.

When de-energized, the valve blocks flow in both directions. The simplicity and appropriate performance characteristics of the valve made it a great choice for use as a semi-active control valve. The area of the orifice of the valve can be varied from 0 to 0.2 in^2 thus allowing up to 0.5 liters/sec of fluid flow. The valve can handle mineral-based or synthetics with lubricating properties at viscosities of 7.4 to 420 mm^2/s. The time response of the valve from fully open to fully closed was between 40-50 ms which is an acceptable time response to allow it to be used as a semi-active damper.

E. Damper construction

The damper consists of several main parts. The tube of the damper houses the standard internal piston. Once assembled, the tube is divided into four chambers: gas, rebound, bypass and compression. The gas chamber is at the top of the tube; it is separated from the compression chamber by a floating piston. This piston

separates the nitrogen in the gas chamber from the oil in the compression chamber. The compression chamber sits between the floating piston of the gas chamber and the piston. The rebound chamber is opposite the compression chamber on the other side of the piston and at the bottom end of the tube. Both chambers are filled with synthetic mineral oil. The piston of the damper is connected to the rod that goes through the rebound chamber and out the bottom of the tube. The rod passes through a special seal designed to keep the oil in, dirt out and to minimize friction between the rod and seal. The two champers are connected to each other through the external bypass valve that is placed externally to the damper. High-pressure hoses are used to connect the SP10-24 valve to the body of the shock. When in compression, the fluid flows through two flow paths, through the internal piston and the external bypass valve. The damping through the internal piston is dictated by the area of the orifices and the stiffness of the shim stack whereas the flow through the bypass valve depends upon the area of the orifice of the valve that is controlled by application of voltage. This takes place the same way but in the opposite direction for the rebound stroke.

A single semi-active damper was fabricated using the components mentioned. The size of the single semi-active damper was kept similar to the size of the passive damper that was purchased so as to obtain equivalent results when tested. This would then be compared to the results obtained for the equivalent passive damper and the double damper.

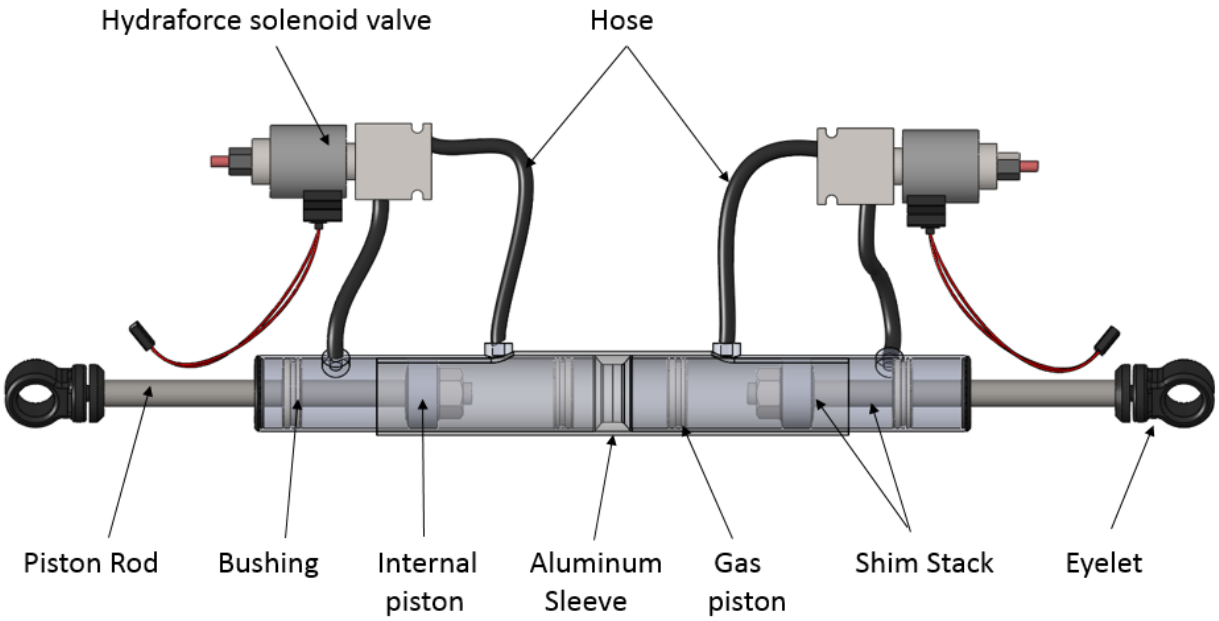

Figure 21: *Final design for double semi-active damper*

The double damper consists of two smaller independent shocks held together with an Aluminum sleeve. The eyelets of the shock were machined off so that both shocks could be assembled against each other. The shocks were then held together in place with the help of one bolt going through each. Additionally, an industrial hose clamp is also used to fasten the shock body to the sleeve. The individual damper constructions are similar to the single shock and essentially just consists of two smaller shocks which add up to the same size. The design of the damper allows splitting the double damper into two individual dampers with ease and allows easy maintenance and service. Moreover both dampers can also be tested individually as will be shown later.

Figure 22: *Dampers used from left to right (a) Fox passive damper (b) Double damper (c) Single semi-active damper*

Chapter 3

Modeling of System

Talbott's [19] and Rhoades' [20] work with mono-tube racing dampers was the basis for the following model. The physical basis of each equation will be explained. Modifications to the method were necessary for modeling of the double damper and flow through the external semi-active valve.

3.1 Damper equations

The damper was broken down into constituents and equations for each part were outlined. All the equations being used will first be mentioned and then the application of the equations on the various dampers will be analyzed separately.

A. Total flow rate

The total flow rate across the piston is the sum of three different flow paths: internal piston flow, external valve flow, and piston leakage flow. The major assumption for summation of flow is that the damper oil is incompressible and therefore has constant density. This assumption allows consideration of volumetric rather than mass flow rates. This is expressed in equation (2). Q is the total volumetric flow rate of the damper in in^3/sec. Q_p is the flow rate through the piston valve, Q_{sa} is the flow rate through the semi-active valve, and Q_{lp} is the flow rate of leakage past the piston seal.

$$Q = Q_{sa} + Q_p + Q_{lp} \qquad (2)$$

The total flow rate Q, through the piston is equal to the change in volume due to the rod side piston area times the velocity.

$$Q = A_r \dot{x} \quad (3)$$

Combining equations (2) and (3) yields a relation among partial flows and velocity.

$$A_r \dot{x} = Q_{sa} + Q_p + Q_{lp} \quad (4)$$

The individual flow rates will need to be established. These flows are all driven by the pressure difference, $\Delta p = p_c - p_r$ between the compression and rebound chambers. A Bernoulli's equation can be used to model unsteady flow through a passage of area A. It has the form:

$$Q = AC_d\sqrt{\frac{2\Delta p}{\rho}} \quad (5)$$

C_d is a steady state discharge coefficient and ρ is the density. C_d is a function of dimensionless parameters including acceleration number, Reynolds number, Cauchy number, and thickness to length ratio and is experimentally obtained. Lang assumed the value for C_d to be constant and found good correlation to experimental data [29]. This model for unsteady flow will be applied to flow in the valves, and will be assumed turbulent based on Reynolds numbers during operation. The flow is turbulent except in the very low speed region. Each component of the equation is then split and modeled separately.

The flow obtained in the damper consists of:

B. Semi-active valve flow (Q_{sa})

The valve is composed of a circular ball detent that allows a change in area from 0 to 0.2 in^2. The valve was modeled as a bleed hole that allowed a constant amount of fluid at any moment. The fluid flow could then be varied based on what voltage condition was being used. A slider was used to vary area based on the input voltage being used. The shape of the indenter is not modeled and the valve is assumed to behave like a normal circular hole.

$$Q_{sa} = A_{sa} C_d \sqrt{\frac{2(p_c - p_r)}{\rho}} \qquad (6)$$

C. Leakage flow (Q_{lp})

The leakage of oil between the piston seal and the cylinder results in a certain amount of fluid flow. Lang modeled this flow using laminar flow through parallel plates [29]. This assumption is valid because the between cylinder seal and wall is very small (<. 004") compared to the length of the flow. The length of the flow is the height of the piston. The equation for this leakage flow is derived from Navier-Stokes equations. The height of the piston is b, while D_p is the diameter of the piston.

$$Q_{lp} = \left(\frac{(p_c - p_r)\, b^3}{12 \mu l} + \dot{x}\frac{b}{2}\right) \pi\, D_p \qquad (7)$$

D. Gas Chamber Modeling

In a mono-tube damper, the gas chamber accounts for the increase of volume

caused by the insertion of the piston rod. Talbott assumed the damper oil was incompressible, which makes the gas pressure a function of the piston displacement. Figure 23 shows the forces acting on the gas piston.

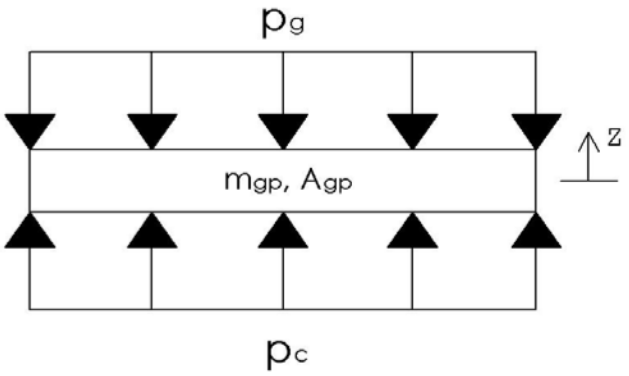

Figure 23: *Free Body Diagram of Gas Piston. Used under Fair Use 2016* [20].

The temperature in the gas chamber usually remains the same, when the damper is operated at one particular operating temperature for short periods of time. Moreover as the oil being used is assumed to be incompressible, the ideal gas law can be used to determine the pressure in the gas chamber and the final volume.

$$V_f = V_i + \Delta V \quad (8)$$

$$p_f = p_i \frac{V_i}{V_f} \quad (9)$$

The gas chamber is modeled as a cylinder and its volume is the product of gas piston area (A_{gp}) and chamber length (L_g). The change in volume is negative for compression and positive for rebound.

$$V_i = A_{gp} L_g \quad (10)$$

$$\Delta V = -A_{rod}\, x = -(A_c - A_r)\, x \qquad (11)$$

If p_g is considered as the gas pressure at a given instant of time and p_{gi} is the initial gas pressure, equations (8) and (9) become:

$$V_f = A_{gp} L_g - (A_c - A_r)\, x \qquad (12)$$

$$p_g = p_{gi} \frac{A_{gp} L_g}{A_{gp} L_g - A_{rod} x} \qquad (13)$$

According to the force balance shown in Figure 24, compression chamber pressure can be found. The summation of forces yields:

$$(p_c - p_g)\, A_{gp} = m_{gp}\, \ddot{z} \qquad (14)$$

$$\ddot{z} = \frac{A_{rod}}{A_{gp}}\, \ddot{x} \qquad (15)$$

Combining equations (13), (14) and (15) gives:

$$p_c = \frac{A_{rod} m_{gp}}{{A_{gp}}^2}\, \ddot{x} + p_{gi} \frac{A_{gp} L_g}{A_{gp} L_g - A_{rod} x} \qquad (16)$$

E. Piston valve flow

Modeling of the flow through the piston is broken down into two parts: flow through the piston orifice and flow contacting the shim stack and exiting. This flow through the shims is referred to as flow through the valves. Two pressure drops are associated with this flow path.

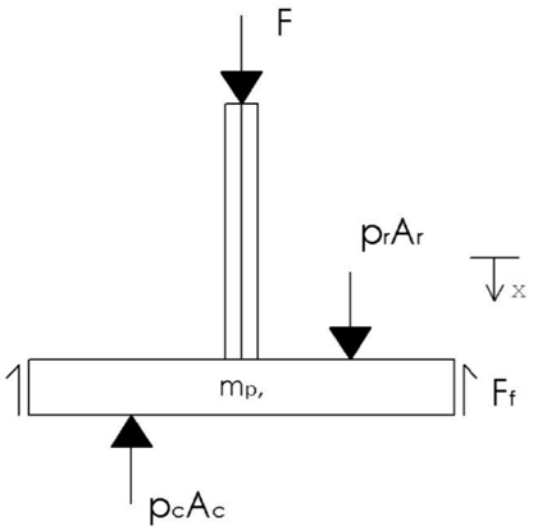

Figure 24: *Free Body Diagram of Piston. Used under Fair Use 2016* [20].

As fluid exits the compression chamber and flows through the piston orifice, the first pressure drop occurs. This is denoted Δp_{po}. The second pressure drop, Δp_{valve}, occurs across the shim stack after the flow has exited the piston orifice. Δp_{po} + Δp_{valve} is equal to ($p_c - p_r$).

$$\Delta p_{valve} = p_v - p_r \quad (17)$$

$$\Delta p_{po} = p_c - p_v \quad (18)$$

Areas of the standard piston were checked by measuring the piston with a vernier and then using a CAD Model to find the areas. The discharge coefficients used were derived from Lang's model.

Once the fluid flow through each of the components has been obtained, this can be used to find out the pressure in the two chambers.

The flow rate through the piston orifice has the same form as the equation used for the semi-active valve.

$$Q_p = A_o C_d \sqrt{\frac{2\Delta p_{po}}{\rho}} \quad (19)$$

The flow through the piston orifice is equal to the flow through valves due to conservation of mass. Valve flow is driven by the pressure drop shown in equation (20).

$$Q_p = A_v C_d \sqrt{\frac{2\Delta p_{valve}}{\rho}} \quad (20)$$

The complexity arises when modeling the A_v term. The flow leaving the piston orifice has contacted the shim stack and essentially turned 90 degrees. For this flow, the flow area is the cylinder wall area defined by the circumference of the shims and height of the shim stack deflection.

$$A_v = \pi D_v y \quad (21)$$

In equation (21), πD_v is the circumference of the largest shim in the damper and y is the shim deflection.

$$Q_p = (\pi D_v y) C_d \sqrt{\frac{2\Delta p_{valve}}{\rho}} \quad (22)$$

The shim deflection y is an unknown in the system of equations. It can be determined from a force balance on the shims itself. The shims are essentially modeled as a linear spring to determine the shim deflection y. The method for finding the stiffness, k will be explained in the Shim Stiffness Modeling section. The relation between deflection and force, ky can be found by a force balance on the valve as shown in figure 25.

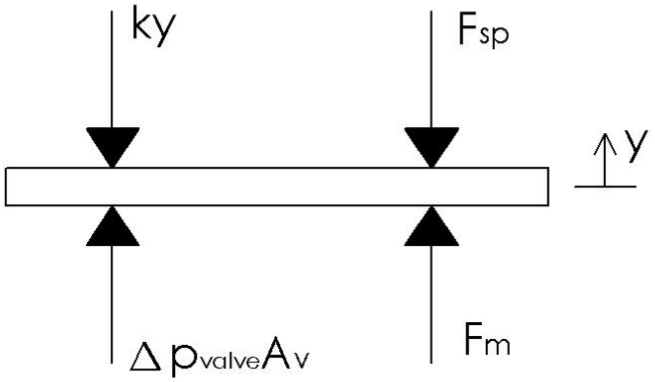

Figure 25: *Free Body Diagram of Shim. Used under Fair Use 2016* [19].

Summing the forces in the y direction gives equation (23).

$$ky = \Delta p\, A_o + F_m \tag{23}$$

The momentum force, F_m, is derived from the conservation of momentum through the valve. This force arises from the 90 degree direction change of the flow in the valve. The momentum equation in the y direction is:

$$F_m = \rho v_{yin} Q_{in} - \rho v_{yout} Q_{out} \tag{24}$$

The velocity out of the valve in the y direction is assumed to be zero, and the velocity in is related to the flow in divided by the area.

$$v_{y,out} = 0 \tag{25}$$

$$v_{y,\,in} = \frac{Q_{in}}{A_o} = \frac{Q_v}{A_o} \tag{26}$$

Combining equations (23) and (24) into equation (26) gives:

$$F_m = \rho \frac{{Q_v}^2}{A_o} \tag{27}$$

According to Lang, a correction factor was found experimentally based on actual versus predicted momentum force. The momentum force coefficient, C_f, was found to have a value of 0.3. Combining C_f with equations (23) and (27) gives:

$$ky = \Delta p_{valve}\, A_v + \rho \frac{{Q_v}^2}{A_o} C_f \qquad (28)$$

Equation (28) is the final force balance on the valve. The deflection can be found if the shim stiffness is known.

F. Shim Stiffness

Deflection of the shim stack in equation is an unknown and is found using a shim stiffness term. Talbott used equations for the deflection of uniform thickness plates, applied superposition to the system, and found the bottom shim deflection from the loads and reaction forces [19]. Rhoades used an FEA model to simulate the deflection being obtained for the shim stack. This approach was used to calculate the deflection being obtained in the FOX Shim stack. SolidWorks models of the different shims were created and the modulus of elasticity, strength and Poisson's ratio for Stainless steel was used in the shim models. Finite element analysis was then performed to find the shim deflection and calculate the shim stiffness.

The pressure loads in the bottom side were applied only at the places where the shim contacted the piston and experienced a force. Tests were carried out for the compression and rebound shim and the maximum deflection for each was analyzed. A pressure of 200 psi was applied and the shim was constrained in the center edge as a fixed boundary. Based on the pressure applied, the force was calculated and the deflection was found accordingly.

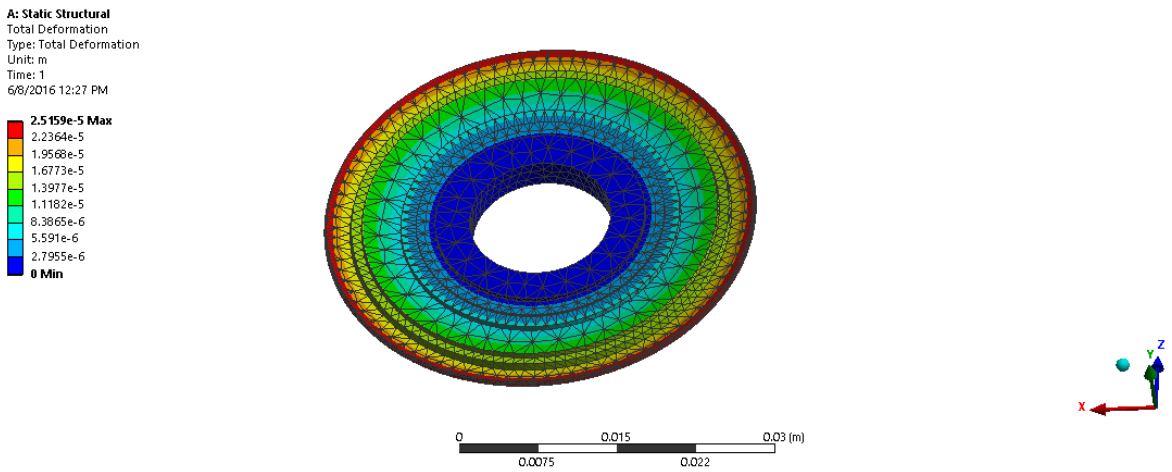

Figure 26: *Deflection of rebound shim stack*

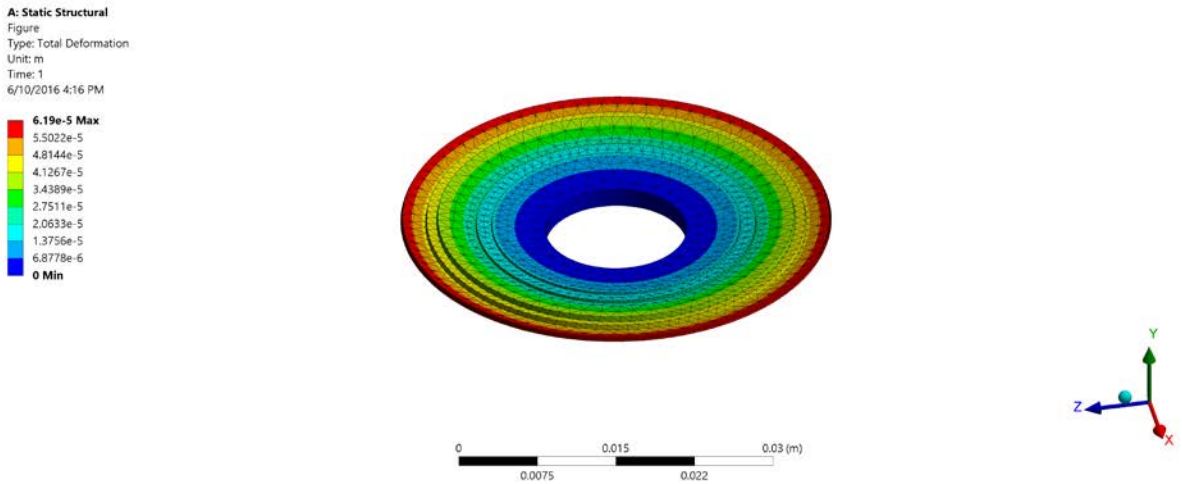

Figure 27: *Deflection of compression shim stack*

It can be seen from the figures 26 and 27 that the deflection being obtained on application of 200 psi is 0.02 mm and 0.06 mm for rebound and compression shim stack respectively. This value was then used as an input to equation (28) to calculate the shim deflection.

G. Damper Force modeling

After the chamber pressures were calculated, the damper force was found. The forces on the damper are as shown:

$$F + p_r A_r - p_c A_c - F_f = m_p \ddot{x} \quad (29)$$

F is the damper shaft force and F_f is the friction force acting on the piston. The acceleration for the input (lower) damper is calculated from the known sinusoidal input from the damper dynamometer and the pressures are calculated from the model above. The mass of the piston assembly, m_p, includes the piston, the rod, bearing and eyelet. The areas are also measured parameters. The friction force, F_f is calculated by the damper dynamometer from measurements made while the piston is moving very slowly so that the pressure difference is negligible. The gas pressure is set to a constant value of 200 psi for all the tests being run. The damper shaft force is then the only unknown and can be determined. For the upper damper in the double damper setup, the acceleration term gets modified as will be seen later.

3.2 Model for damper

All of the equations formulated were used for both the passive and double damper independently. A Simulink model was created for each of them and Newton's iterative method was used to solve the non-linear equations obtained.

A. Model for single passive damper

There are six unknowns according to the equations in the model. Certain characteristics of the damper were measured whereas others were experimentally evaluated. As the single passive damper consists of one internal piston, Equations (4), (6), (7), (16), (22), (28) were used for the model. The difference in the equations being that the passive damper did not include the semi-active orifice fluid flow. Therefore equation (6) was ignored and equation (4) was modified to:

$$A_r\dot{x} = Q_p + Q_{lp}$$

B. Model for double damper

The equations mentioned for the single damper formed the basis for the model of the double damper. Two individual dampers were modeled with similar properties. The two dampers were then assumed connected to each other rigidly at the interface. This meant that a certain component of the force and velocity being experienced by the lower damper would be transmitted to the upper damper and vice versa. Moreover there were a total of three parts now, the lower damper, the body and the upper damper. The lower damper would be excited by the dyno which based on the amount force being applied and the resistance being offered by the lower and upper piston, would transmit a certain component of its force to excite the body connecting the two pistons. The force is a function of the velocity and displacement of the input, the relative pressures and cross sectional areas of the chambers and the direction of the stroke. These can all be linked by the resultant force the damper experiences at the eyelet as defined by Equation (30). A correction

factor γ would be used to validate the model based on the experimental data obtained. Therefore the force connecting the two dampers was defined as:

$$F_{upper\_input} = \gamma F_{lower} = m_{body} (\ddot{x}_{body}) \quad (30)$$

where m_{body} is the combines mass of the aluminum sleeve and the two damper bodies and $\ddot{x}_{body}$ is the induced acceleration due to the input. F_{lower} is the resultant damping force experienced due to the internal fluid of the lower damper and γ is a correctional factor used to correlate the force found by experimental testing.

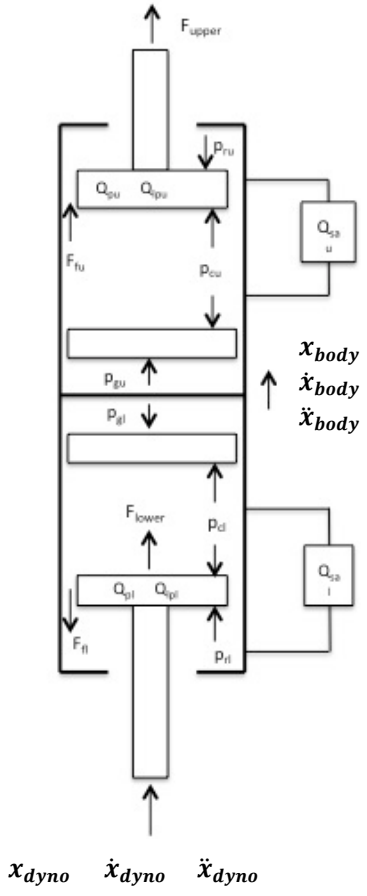

Figure 28: *Free body diagram of double damper*

The force thus transmitted $\boldsymbol{F_{upper\_input}}$ was used as an input to the upper damper. This then essentially forms its own damper system and faces a resistive force as mentioned in equation (29). The force input from the lower damper to the upper damper has a threshold mark based on the resistance faced in the upper damper and the relative accelerations of the lower damper and body. The upper damper would start moving once the input force to the lower damper overcomes the resistance force of the upper damper. The force balance for the upper and lower damper can thus be defined as:

$$F_{lower} + p_{rl} A_{rl} - p_{cl} A_{cl} - F_{fl} = m_{pl} (\ddot{x}_{dyno}) \quad (31)$$

$$F_{upper} + p_{ru} A_{ru} - p_{cu} A_{cu} - F_{fu} = m_{body} (\ddot{x}_{body}) = \gamma F_{lower} \quad (32)$$

The acceleration of the sleeve of the damper, $\ddot{x}_{body}$ thus obtained will be the resultant acceleration of the mid-section that is created due to the resistive force being offered by the lower piston and upper piston. Since $\ddot{x}_{dyno}$ is known, the acceleration obtained can then be integrated to obtain a velocity and displacement input for the piston in the upper damper.

The two forces can thus be equated to obtain the force the dyno finally records:

$$F_{upper} = \gamma m_{pl}(\ddot{x}_{dyno}) - (p_{ru}A_{ru} - p_{cu}A_{cu} - F_{fu}) - \gamma(p_{rl} A_{rl} - p_{cl}A_{cl} - F_{fl}) \quad (33)$$

The force v/s velocity plots thus can be generated by using the equation (33). The force F_{upper} is the force measured by the load cell and is the final force used for plotting the damper curves. Based on the equation it can be seen that, the damper

can essentially be modeled as a single damper that has two pressure and rebound chambers. But to be able to estimate the fluid flow and pressure change due to each component is analyzed and all the equations used are shown in Table 1.

The two dampers in the model had variable sliders that allowed the orifice area of the semi-active valve in either case to be varied. The model was created as an iterative loop in Simulink and a time step of 100 seconds was used to solve the equations. The parameters were all input into Matlab, and Simulink was used to create and run the whole model.

Table 1: *Equations used for double damper model*

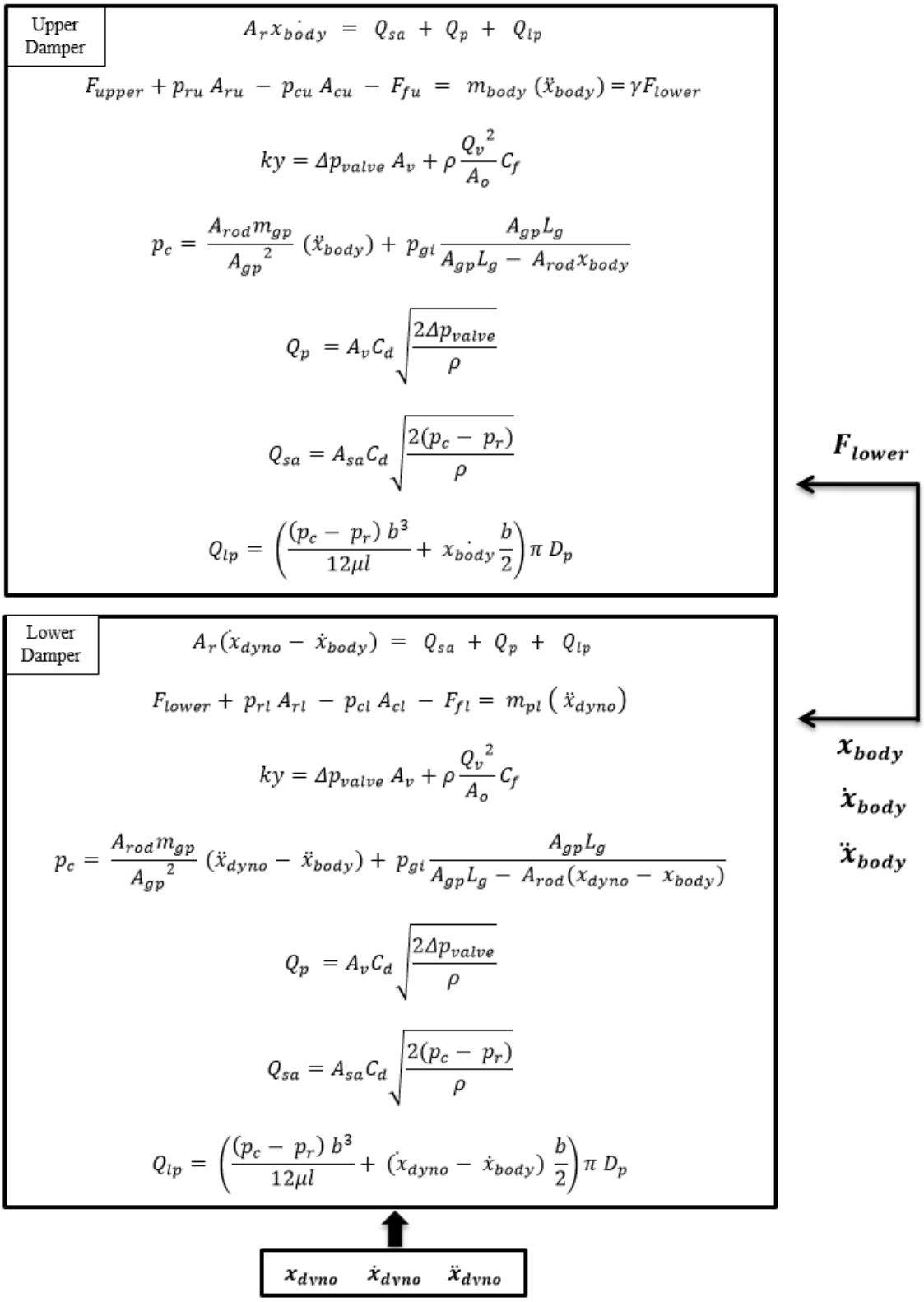

Chapter 4

Testing

Two dampers were fabricated and tested. Both the single semi-active and double semi-active dampers were equipped with the standard pistons and solid pistons and were tested on a shock dynamometer to obtain Force v/s velocity curves at different speeds.

4.1 Experimental test equipment

Real damper testing was conducted to obtain experimental data on damper force characteristics. The double damper was tested on an Intercomp 2 HP Dynamometer as shown in figure 29. The data for the dyno comes from a transducer which measures the input RPM of the motor. The stroke of the cycle is fixed by adjusting the scotch yolk mechanism manually. The forces being experienced on the eyelet are measured by a load cell that comes fitted on to the shock dyno. The Intercomp dyno also comes with software which generates force v/s velocity and force v/s displacement curves and allows collection of data points for the test. Custom Aluminum bushings were machined as the bushings obtained with the damper were made out of Nitrile rubber and deformed when a force was applied, thus giving inaccurate force readings.

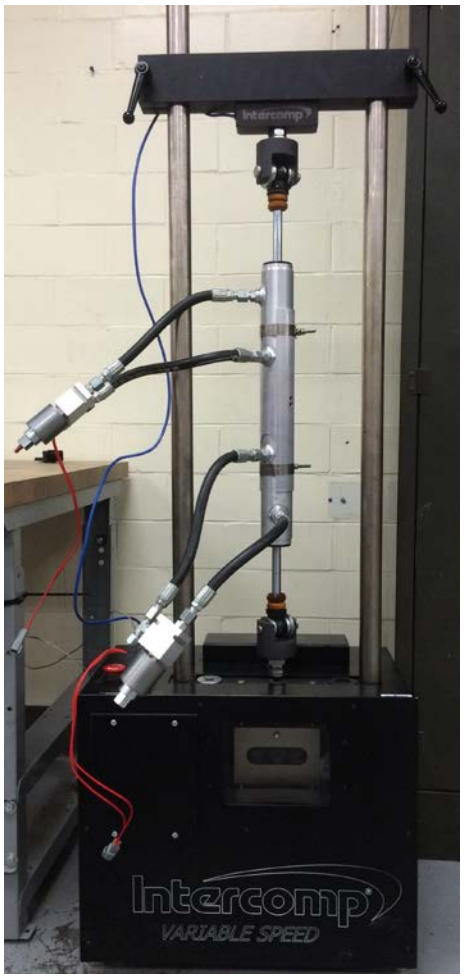

Figure 29: *Double damper mounted to Intercomp Dyno*

To test the semi-active damper, an electrical circuit as shown in figure 30 was setup. An EVDR Controller provided by Hydraforce was used to interface the solenoid valve with an NI DAQ that was responsible for providing an input voltage to the controller. A 12 V power supply was used to maintain the supply voltage and the shock was provided an input from 0-5V that corresponded to a change in area of the orifice. An input voltage of 5 V thus created a current of up to 1.2 A at which the point the valve completely open. The data points from the tests of the dyno were recorded by the Intercomp software and were then exported to Excel.

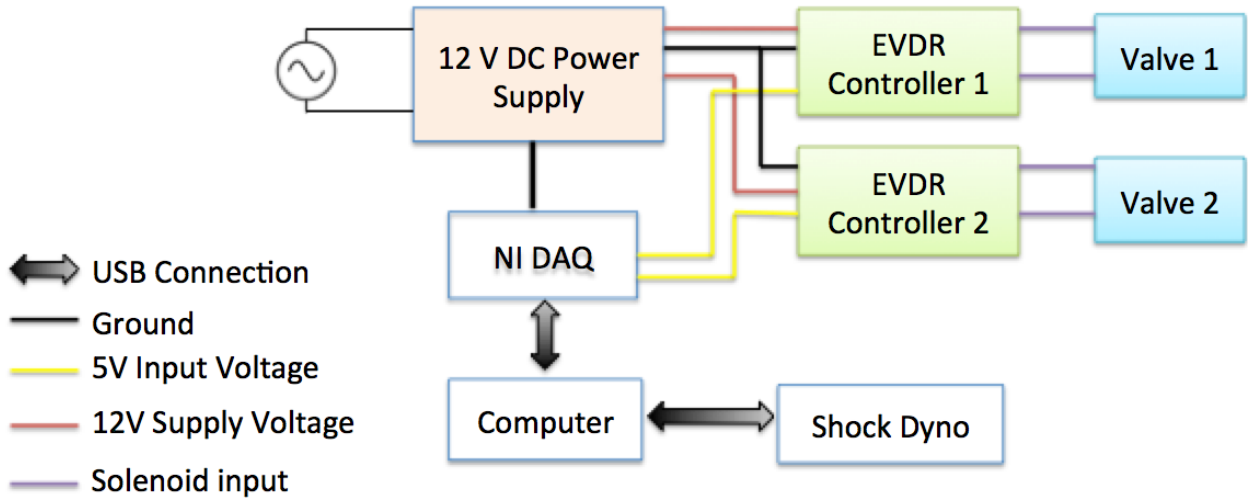

Figure 30: *Test Setup*

The input voltage is provided by the NI DAQ which is controlled using LabView. A change in voltage in LabView would correspond to a change in current of the power supply and thus opened or closed the valve accordingly. An input voltage of 5V corresponds to the valve being fully open and 0 V corresponds to the valve remaining fully closed. The current for the valve varies from 0 to 1.2 A after which the controller cuts off any input to the valve. When the solid piston was tested, a voltage lower than 0.5 V was not used as that created excessive pressure on the shock body.

The shock dyno software is used to input the desired test velocity. A stroke length of 2” was used for all the tests and the velocity input was adjusted between 2 and 13 in/sec.

4.2 Testing Method

A series of tests were performed on the single and double semi-active dampers. The double damper is constituted of two smaller single semi-active dampers and these were first tested at low speeds to see the response. The small single semi-active

dampers were tested in two configurations, with a solid piston and a standard piston with a symmetric shim stack. This allowed us to see the response of using different pistons. After this, a passive damper and single semi-active damper of the same size were tested. Three tests corresponding to 1 V/ 0 A, 3 V/ 0.6 A and 5 V/ 1.2 A were run. These values corresponded to the valve being fully closed, half open and fully open. Each current combination was then tested for 4 in/sec, 8 in/sec and 13 in/sec. The passive and single semi-active dampers were tested at 4 in/sec, 8 in/sec and 13 in/sec. Each damper was tested for a low speed friction cycle to find the experimental value of the friction force that was then used as input to the model.

The double damper was tested with multiple current configurations. The damper was tested for three speeds, 4 in/sec, 8 in/sec and 13 in/sec and each speed was tested for different current combinations as shown below.

Table 2: *Current combination used for double damper tests*

Current (in Amperes)		
Combination	**Lower**	**Upper**
11	0	0
13	0	0.6
31	0.6	0
33	0.6	0.6
35	0.6	1.2
53	1.2	0.6
55	1.2	1.2

The current combinations shown are later used to refer to certain tests being performed. “11” refers to both, the lower and upper damper being set to 1 V/ 0 A (fully closed) and 55 refers to both damper being fully open, 5 V/ 1.2 A.

The temperature of all the tests was regulated and all tests were performed at a damper temperature corresponding to $25°C$. The damper was allowed to cool between each cycle and the temperature was measured using a thermocouple mounted directly to the body of the damper. A gas pressure of 200 psi was used for each damper that was tested.

The results obtained from the single semi-active damper, passive damper and the double damper were then compared to each other as shown in Chapter 5.

Chapter 5

Results

This section details the various tests performed and the results obtained. The output graphs that are analyzed are force v/s velocity and force v/s displacement. The results for each test are mentioned and are discussed in detail.

5.1 Single Semi-active Damper

As mentioned, the double damper consists of two single semi-active dampers which were tested for two configurations, solid piston and standard piston. Doing so, individual flow through each piston was also checked for and the differences in response were analyzed.

A. Standard Piston

A standard FOX Piston with a symmetric shim stack was used. The compression shim stack was used as it had a lower stiffness value. The flow through the shock was thus a result of the flow through the piston and the Hydraforce bypass valve. The results obtained when the shock was tested 2 in/sec and 5in/sec for an input voltage/ current of 1 V/ 0 A, 3 V/ 0.6 A and 5 V/ 1.2 A are as shown.

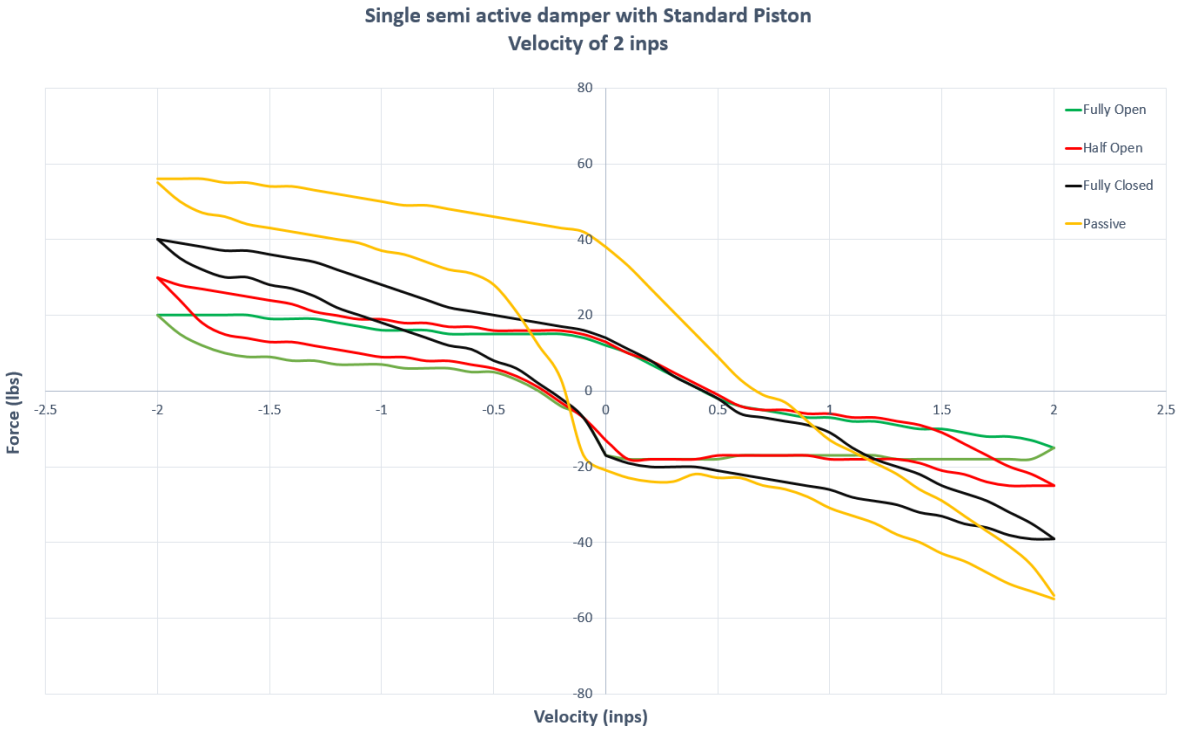

Figure 31: *Single semi-active damper with standard piston compared to equivalent passive damper at 2 in/sec*

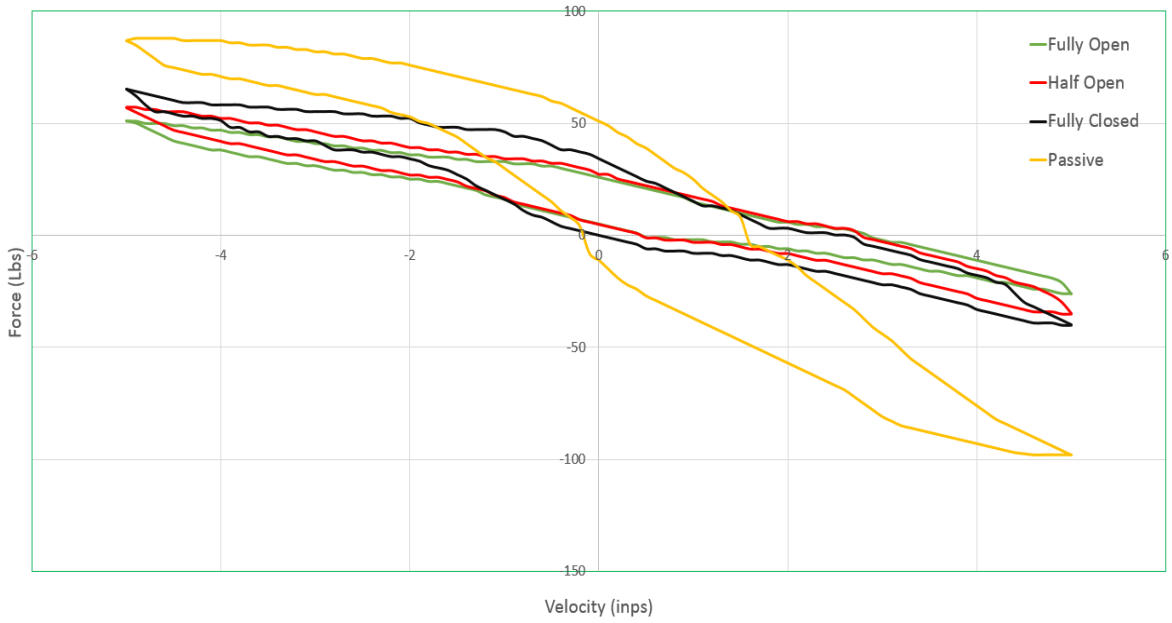

Figure 32: *Single semi-active suspension with standard piston compared to equivalent passive damper at 5 in/sec*

It can be seen from the results that the damper behaves in a fairly predictable manner when voltage is applied. The forces acting on the damper change with velocity due to the combined effect of the shim stack and the semi-active orifice. It can also be seen that the force acting on the damper increases with a decrease in voltage. The forces obtained in the rebound stroke and compression stroke of the damper are numerically similar owing to the symmetric shim stack being used.

The hysteresis curve obtained is similar to that seen in the passive shock. But it can be seen that the forces being produced are much lower than that of the passive shock. This is owing to the fact that the bypass valve is working in parallel with the standard piston thus resulting in lower pressures in compression and rebound. The production damper also showed similar forces in compression and rebound owing to the symmetric shim stack being used.

B. Solid Piston

The internal standard piston of the shock was then replaced with a solid piston that had a small bleed hole so as to act as a fail-safe mechanism during the condition that the solenoid stopped operating. The bleed hole was 0.5 mm in diameter and therefore would have a fair amount of impact on the damping forces being produced but this was done so as to make sure no drastic change in pressure occurred in the damper. The damper was then tested for three input voltages 1 V/ 0 A, 3 V/ 0.6 A and 5 V/ 1.2 A. The results of the tests obtained at 2 in/sec and 5 in/sec are as shown below.

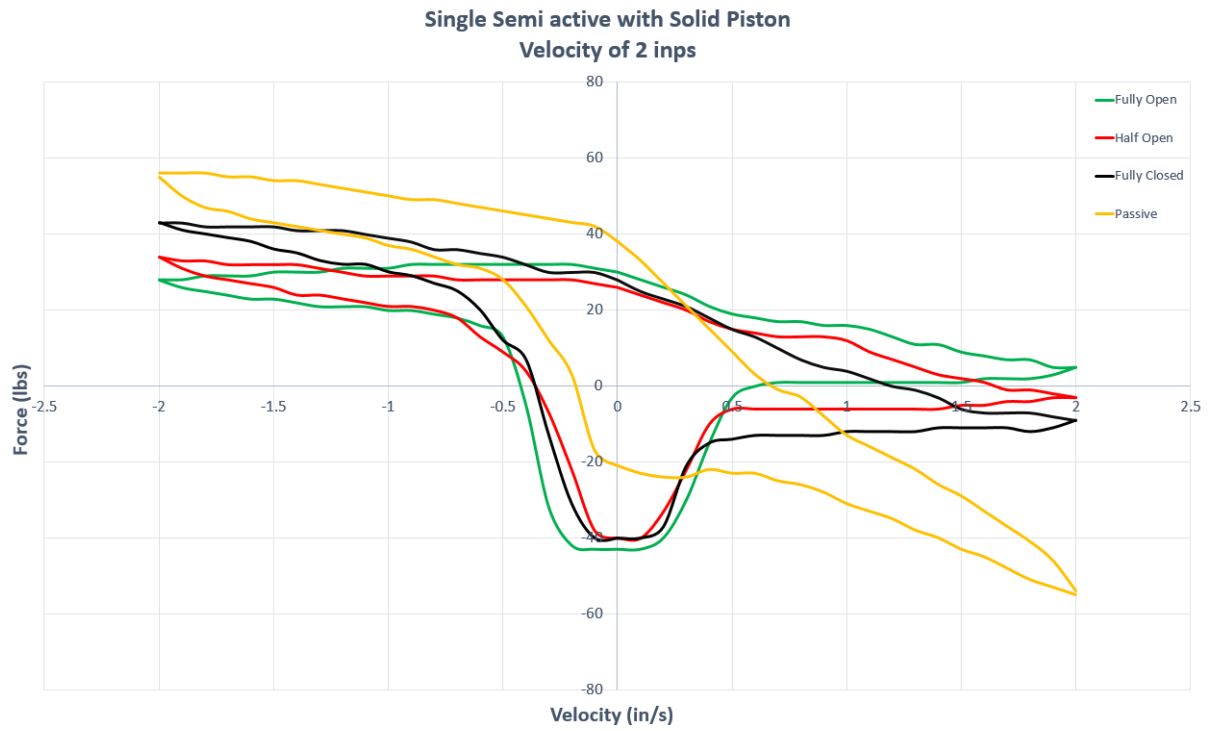

Figure 33: *Semi-active damper with solid piston compared to equivalent passive damper at 2 in/sec*

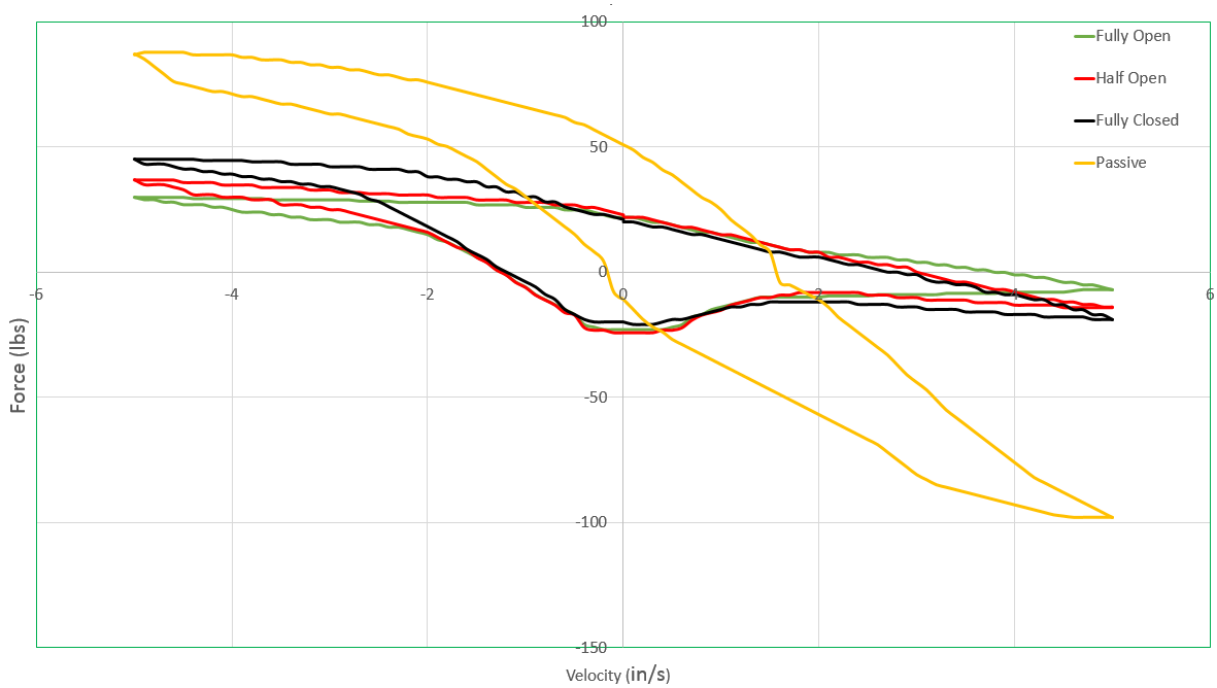

Figure 34: *Single semi-active damper with solid piston compared to equivalent passive damper at 5 in/sec*

From the tests, it can be seen that the forces experienced by the damper are not as expected. A huge spike in force was noticed around 0 in/sec and the forces obtained in rebound were positive. This was attributed to the nature of the piston and setup. The piston being solid, experiences great amount of friction and resistance at the end of its stroke that thus results in an excessive amount of buildup of pressure. This also results in a complete drop in force as the piston moves away from the end of the stroke and thus causes a steep decline in the force being observed. This then results in positive forces to occur as the piston regains speed in rebound. Moreover no bleed shim was used and therefore the linearity in the response at low speeds was lost. From the results, it was also observed that the response obtained was very constant towards the end of the stroke due to the absence of a shim stack to add any resistance. The curve being obtained has a lower slope than the one seen for the standard piston and that is owing to the fluid flow taking place due to the shim stack. It was also seen that the force did change with voltage in a predictable manner with the lowest applied voltage creating the highest amount of force.

These forces were then compared to that of a passive damper. The forces experienced in both strokes are lower than the forces experienced in a standard passive damper. This was attributed to the fact that the combined area of the bleed hole in the solid piston and the semi-active valve was still greater than the area being exposed when the passive damper was in motion. This is because the damper is being tested at lower speeds and therefore the shim stack only exposes a partial amount of the piston during its stroke and therefore does not allow enough damping to take place.

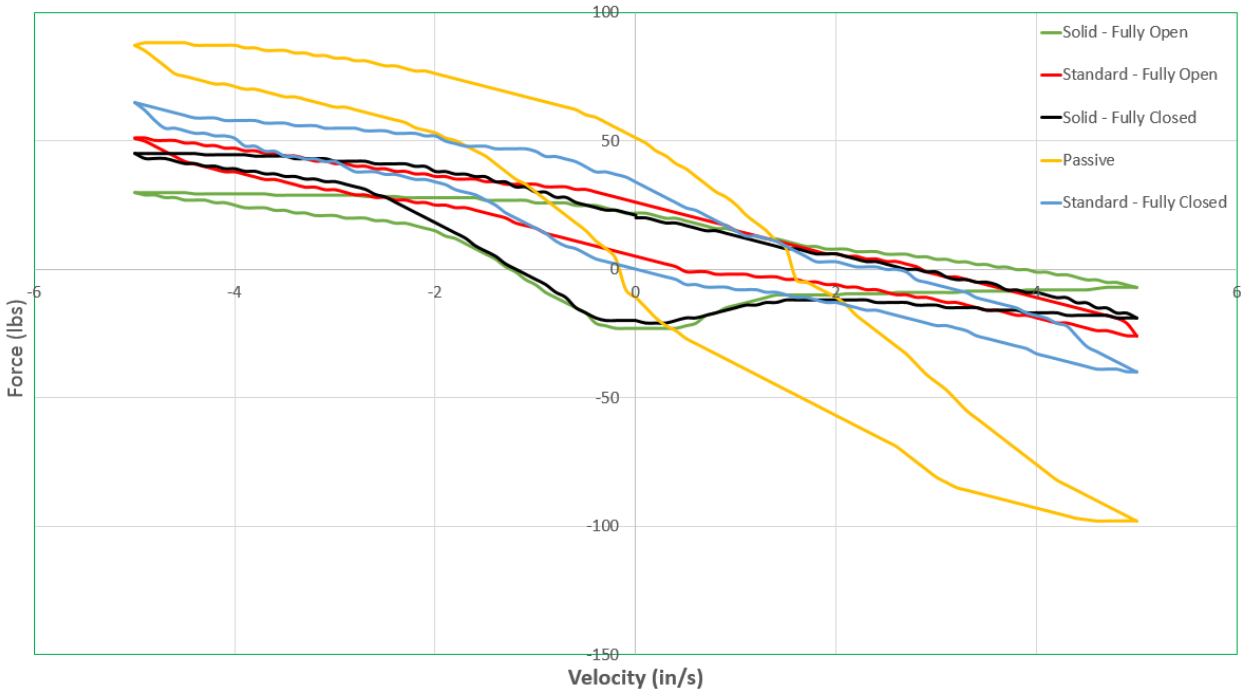

Figure 35: *Single semi-active damper with standard and solid piston being compared to passive damper at 5 in/sec*

As seen, the semi-active damper with the standard piston observes higher forces than the solid piston owing to the bleed hole being machined. Based on the hysteresis curve and the positive forces observed while using the solid piston, it was decided to use the standard piston in both dampers when testing the double damper.

5.2 Double damper

The double damper was tested for multiple speeds and various different voltage combinations as mentioned earlier. Tests were performed at 4 in/sec, 8 in/sec and 13 in/sec.

A. Velocity of 4 in/sec

The valve was progressively opened as mentioned and the following results were obtained.

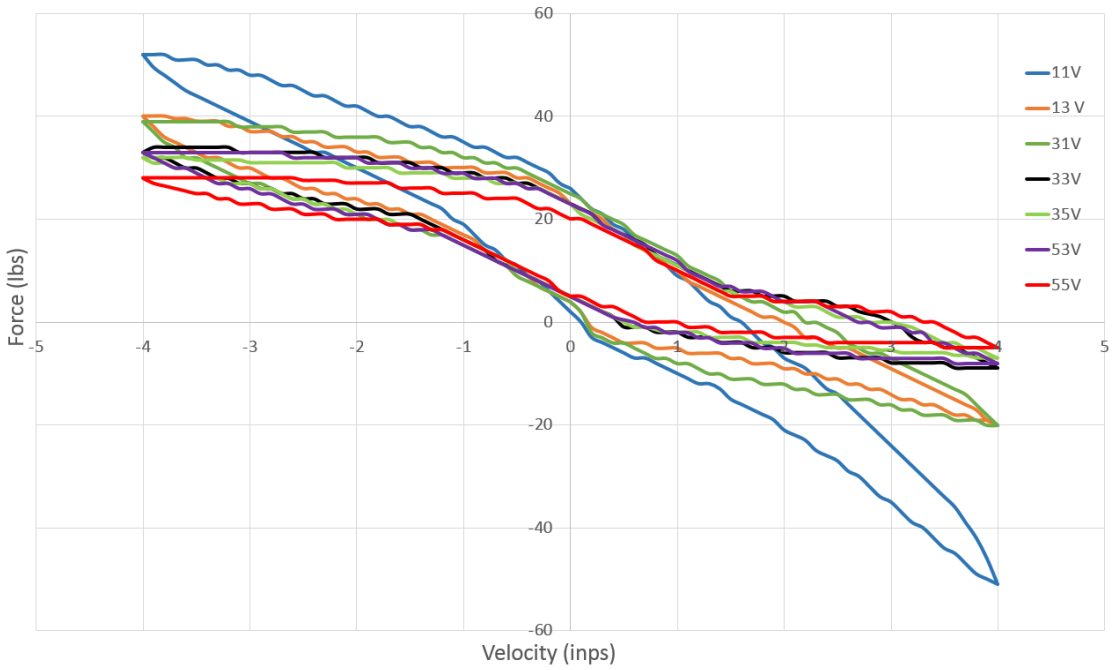

Figure 36: *Double damper tested with valves at different voltage combinations*

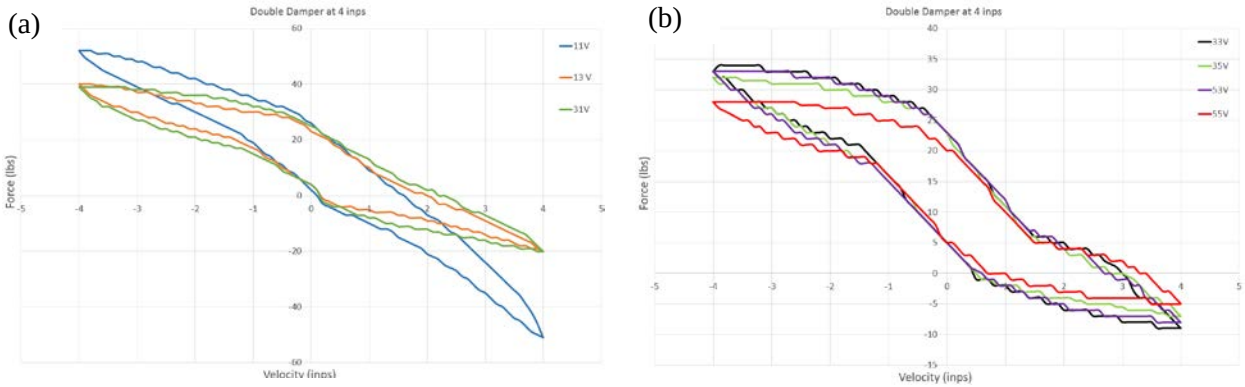

Figure 37: *Double damper results for 4 in/sec at (a) 1-1, 1-3 and 3-1 (b) 3-3, 3-5, 5-3 and 5-5*

Shown above are the results for the various changes in current. It can be seen from the graph that as input current is increased, the force observed at the load cell reduces. The graph follows the trend observed for a normal passive damper with force reducing proportional to velocity in compression and rebound. The hysteresis loop observed for both dampers around 0 in/sec is seen to be similar for all dampers. Also, the forces obtained for the combination of the dampers when the upper damper is fully closed and the lower damper is fully open are observed to be the same as when the upper damper is fully open and the lower damper is fully closed with minor variations in the slopes of the curves.

The double damper when fully open at lower speeds sees higher compression forces than rebound. The damper curve shape does not perform similar to the single passive damper but sees more digressive nature which is because of the fixed flow semi-active valve, higher friction due to bodies and no activation of the shim stack. The knee in the graph is due to the flow through the bleed shim of the shim stack and only happens during the start of the cycle after which flow is taken up by the flow through the fixed semi active valve. When the two valves are completely closed at low speeds, the double damper's force v/s velocity shape more closely resembles that of a single passive as the shim stack is now responsible for majority of the fluid restriction. The graph is more linear in nature which corresponds to both shim stacks being responsible for the fluid flow. The forces obtained in rebound and compression are very similar because the progressive shim of the rebound shim stack has not been activated due to the presence of two dampers. In the passive damper, the slope of the graph in rebound changes after 2 in/sec but this is not observed for the double damper primarily because the fluid flow splits between the two dampers.

(a)

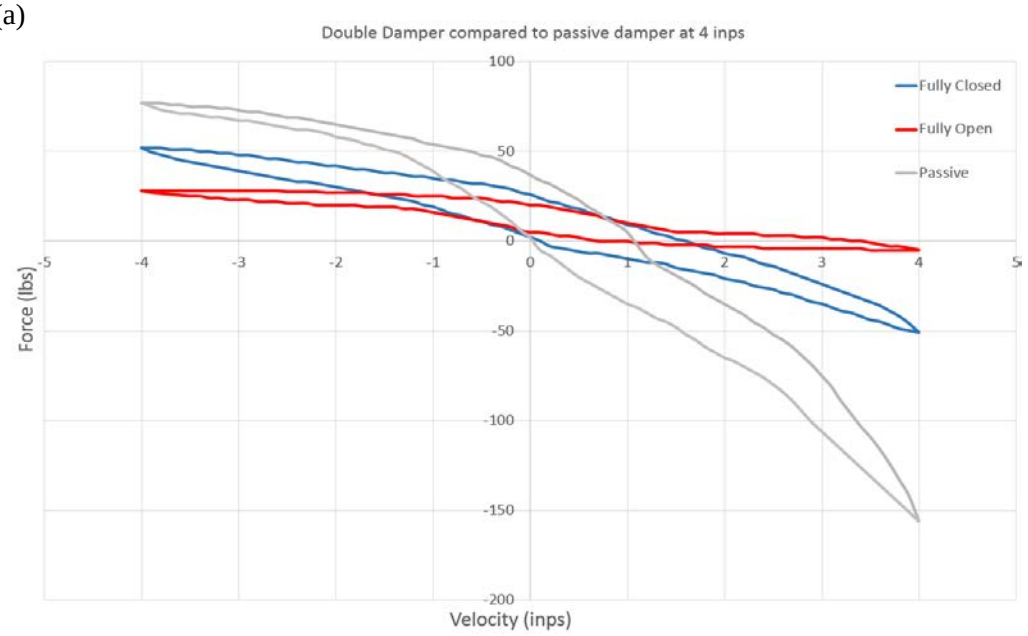

(b)

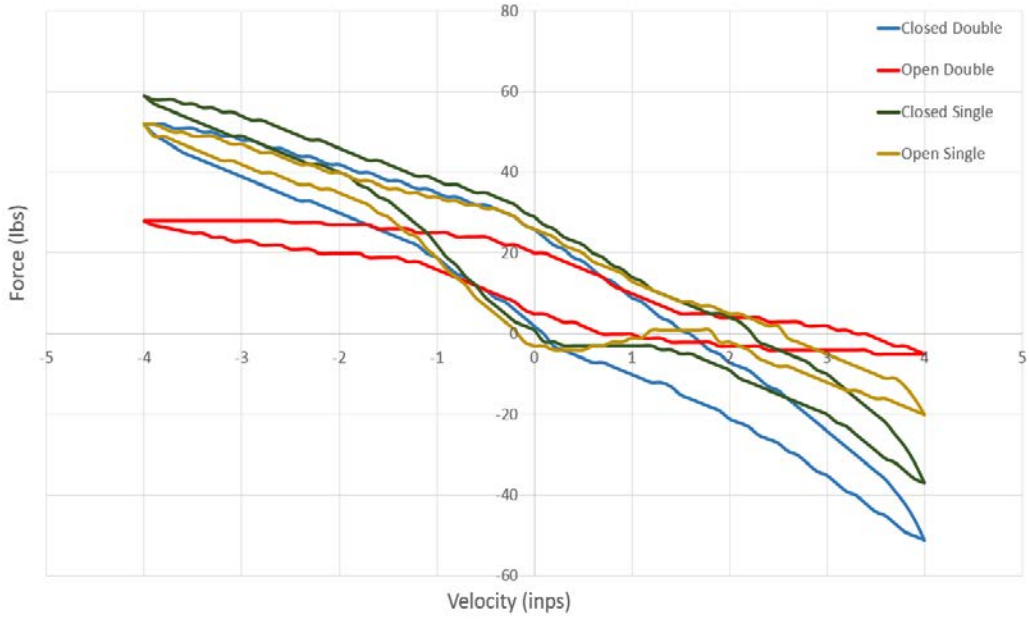

Figure 38: *Double damper results for 4 in/sec compared to equivalent (a) passive damper (b) Semi-active damper*

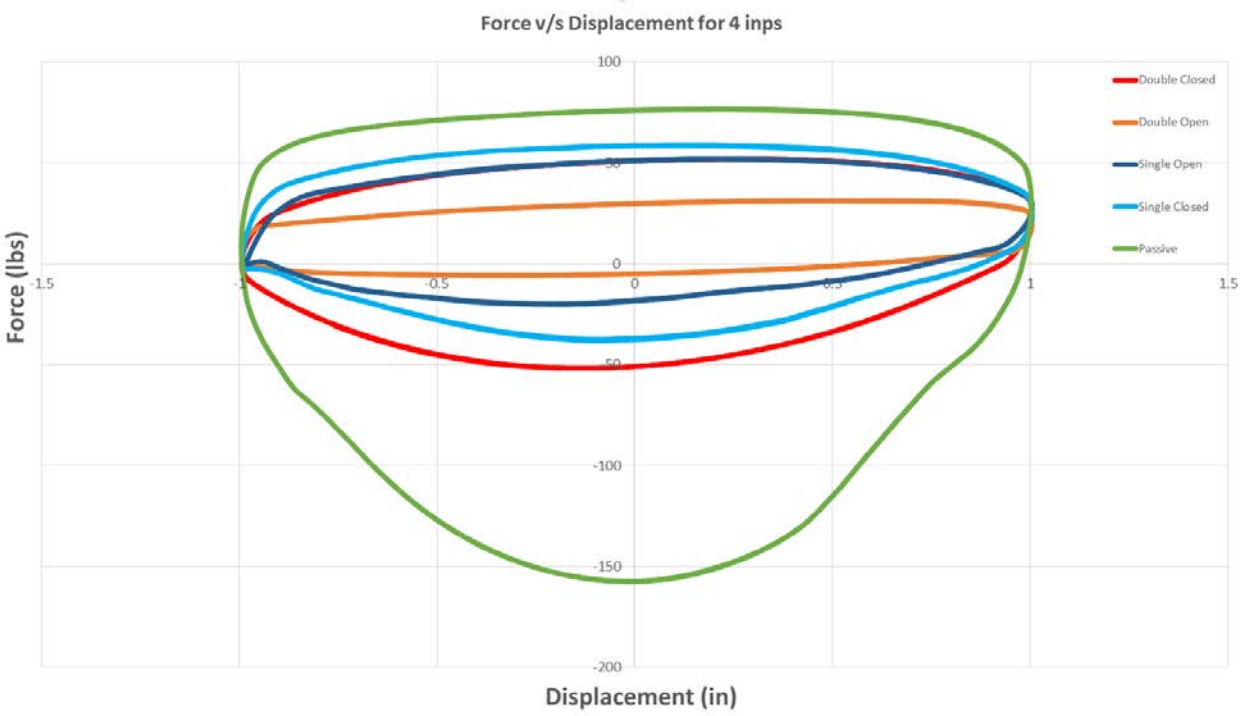

Figure 39: *Comparison of force v/s displacement curves of three dampers at 4 in/sec 2 in stroke*

It can be seen that the forces obtained for the passive damper are much greater in magnitude when compared to the semi-active damper. A reduction of up to 140 lbs of force can be observed in rebound and up to 50 lbs in compression. This entails that if the shim stack can be sized correctly, a large variation in damping can thus be obtained by using the double damper. The forces obtained when compared to the single semi-active damper have a much greater variation. The single damper has a greater compression force when fully closed whereas the double damper observes a much greater force in rebound. The single semi-active damper has only one shim stack which does not open much in compression as the test is being performed at lower velocities thus resulting in higher forces being obtained. It is also observed that the friction force for both dampers is fairly high thus resulting in a very low rebound force for the double damper when the valve is fully open.

B. Velocity of 8 in/sec

The valve was progressively opened as mentioned and the following results were obtained.

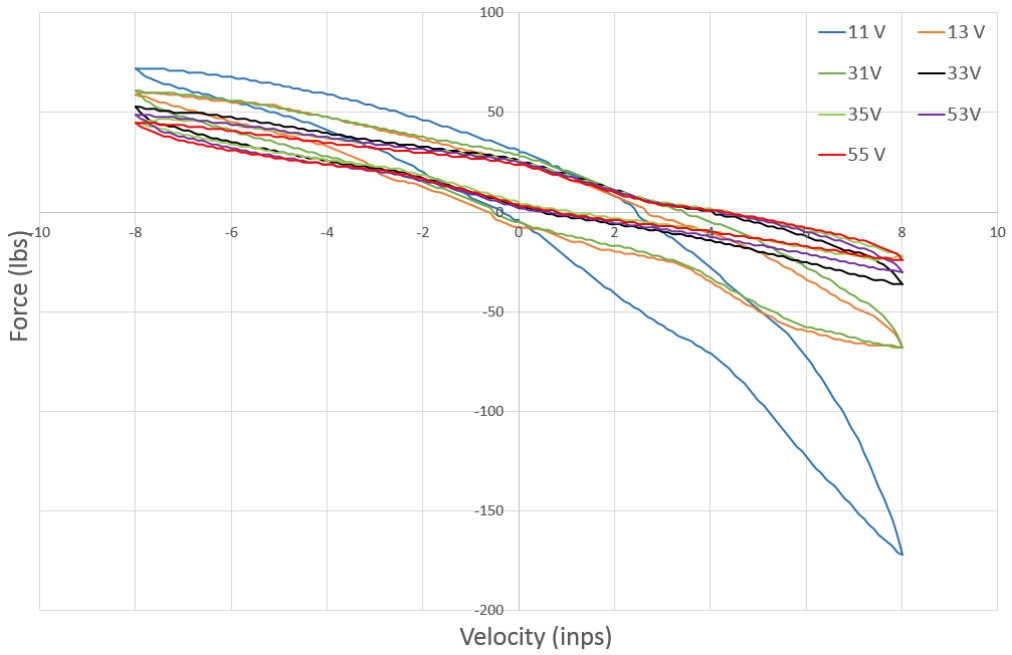

Figure 40: *Double damper tested at 8 in/sec for multiple voltage inputs*

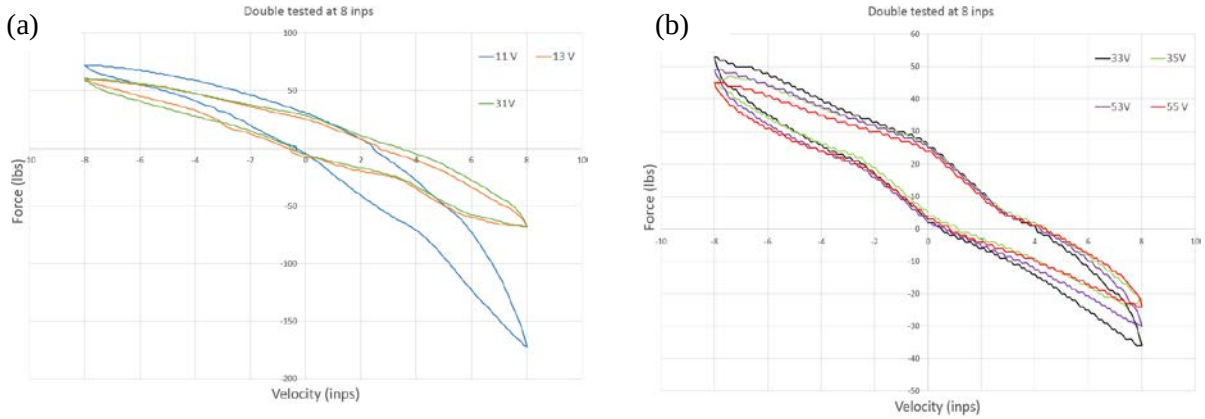

Figure 41: *Double damper results for 8 in/sec for: (a) 1-1, 1-3 and 3-1 (b) 3-3, 5-3, 3-5 and 5-5*

(a)

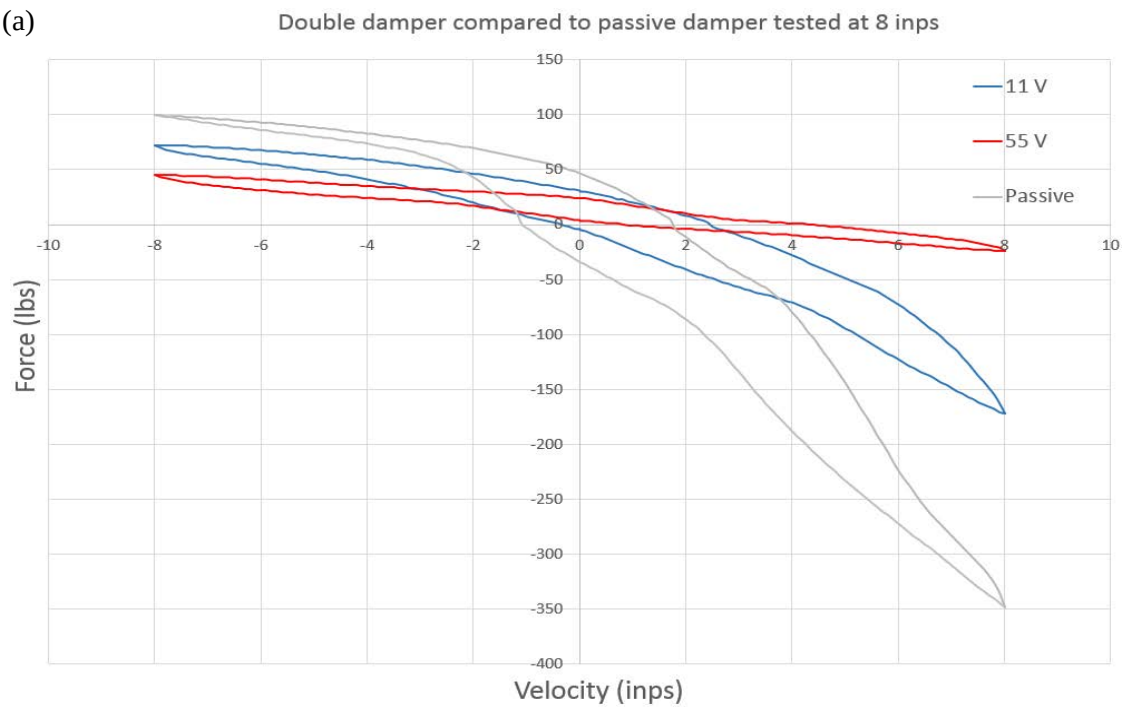

(b)

Figure 42: *Double damper at 8 in/sec compared to equivalent (a) passive damper (b) semi-active damper*

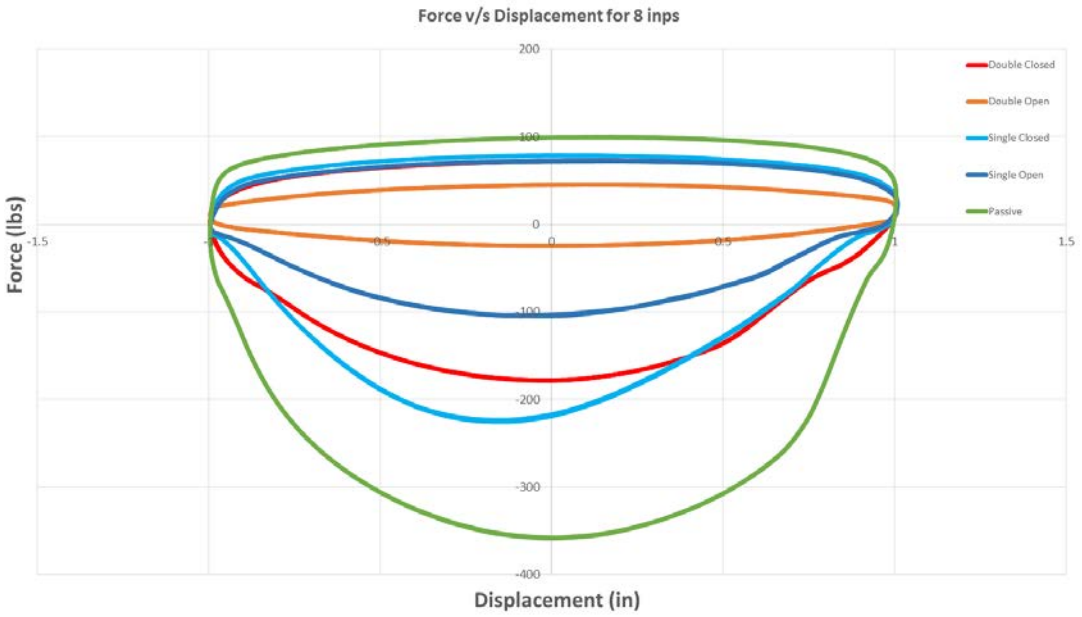

Figure 43: *Comparison of Force v/s displacement curves of three dampers at 8 in/sec 2 in stroke*

C. Velocity of 13 in/sec

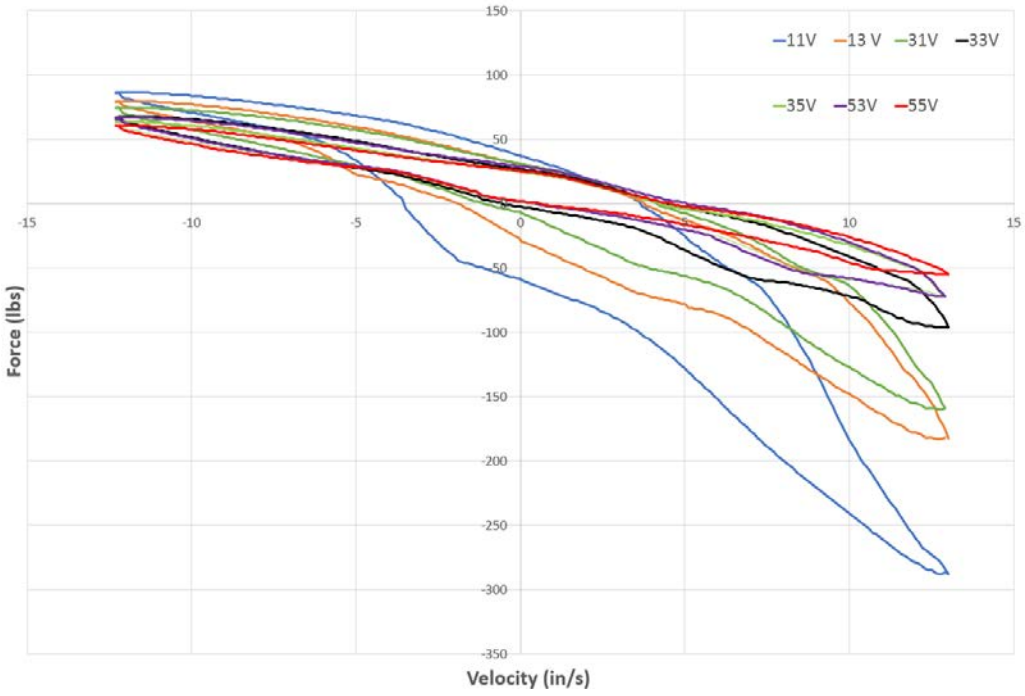

Figure 44: *Double damper tested for multiple voltages at 13 in/sec*

(a)

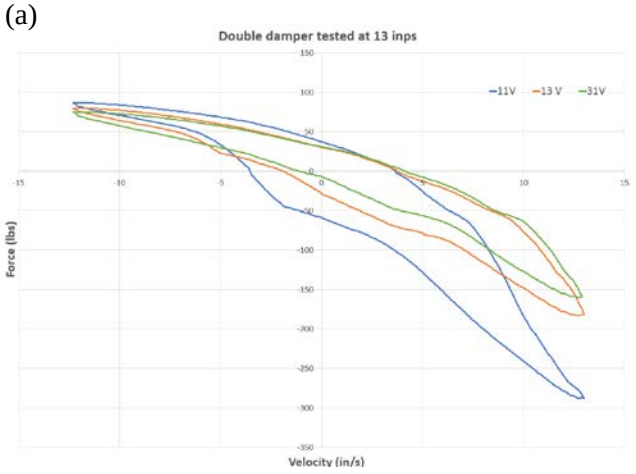

(b)

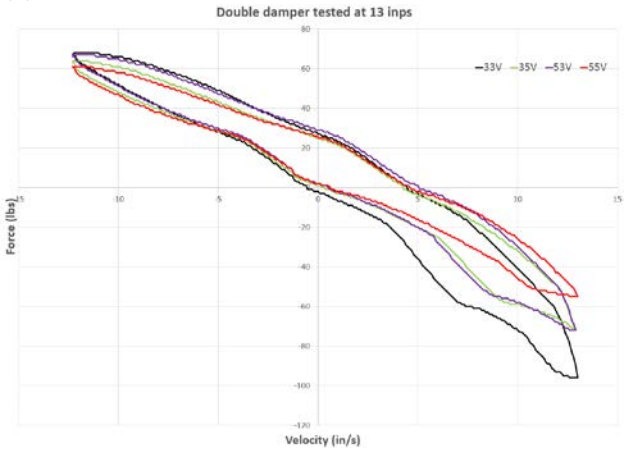

Figure 45: *Double damper results for 13 in/sec for: (a) 1-1, 1-3 and 3-1 (b) 3-3, 5-3, 3-5 and 5-5*

(a)

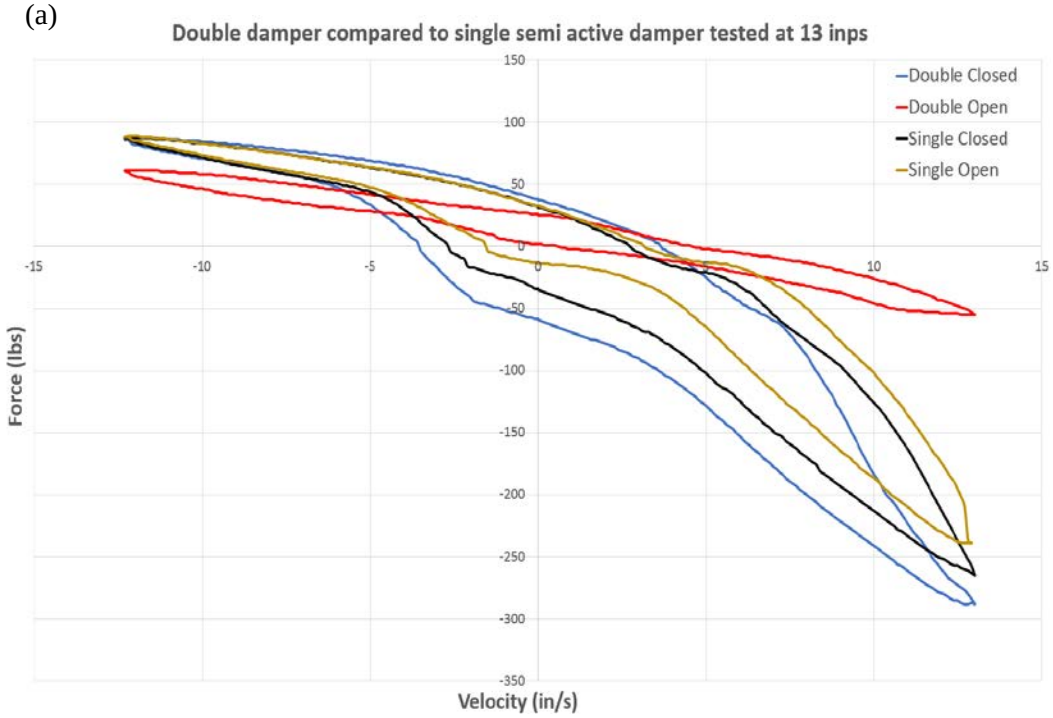

(b)

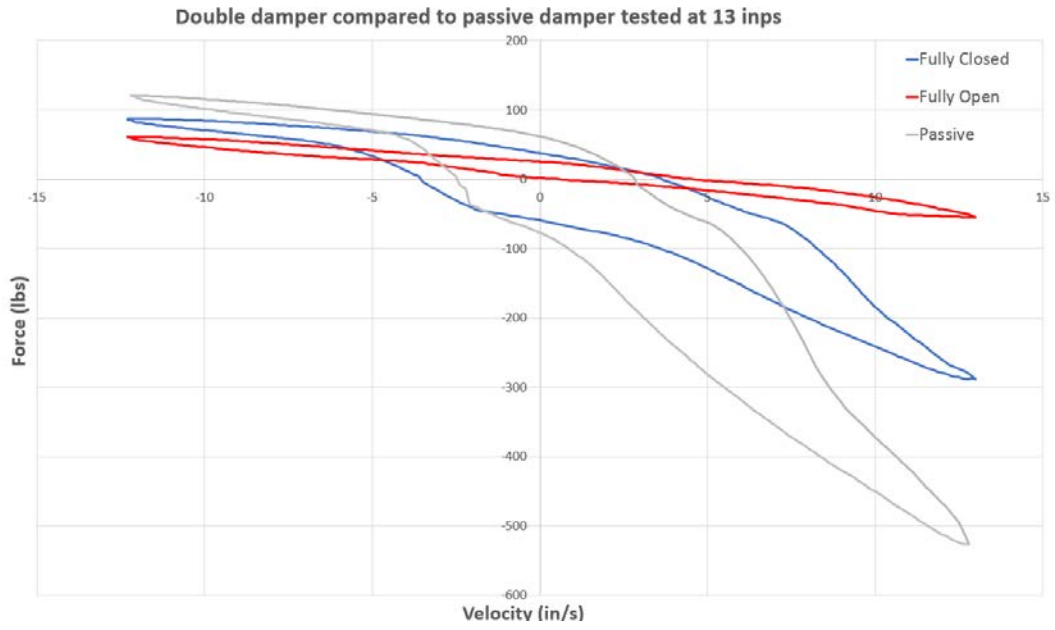

Figure 46: *Double damper at 13 in/sec compared to equivalent (a) passive damper (b) semi-active damper*

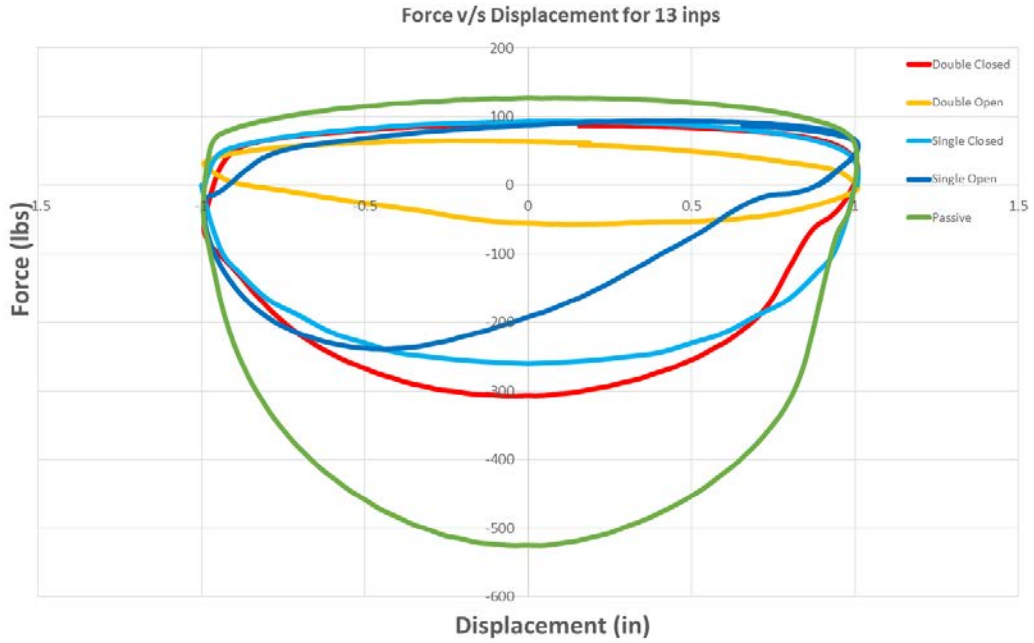

Figure 47: *Comparison of Force v/s displacement curves of three dampers at 13 in/sec 2 in stroke*

The force obtained at 8 in/sec and 13 in/sec follows the same trend as outlined above for 4 in/sec. The force increases with voltage, with rebound increasing much more than compression due to the shim stack. The variation in force obtained for the double damper is much higher than that obtained for the single semi-active or passive damper.

The result for the double damper at higher speeds when fully open were as expected. The region around 0 in/sec corresponds to flow through the bleed shim and semi active orifice. The slope after around 4 in/sec remains almost the same as this too corresponds to flow mainly taking place through the semi active valve as a result of which the force just linearly goes on increasing.

At higher speeds, the double damper with both valves closed starts more closely resembling the single passive damper results. The shape of the rebound and compression curve is more similar to the double damper due to the two valves being closed and all the fluid flow taking place due to the complete opening and closing of the shim stack. The transition in the curve that takes place when the damper switches from compression to rebound can also be seen around 0 in/sec which is similar to what we see for the Fox damper. Moreover the change in slope due to the shim stack completely opening can also be observed for the rebound stroke.

5.3 Model correlation

The damper model as mentioned in Section 3 is now compared to the results obtained for the tests of the double damper. The Force v/s velocity curves for the

double damper are compared with the model for the normally open and normally closed position. Also, the model for a single damper is compared to the tests for the passive damper.

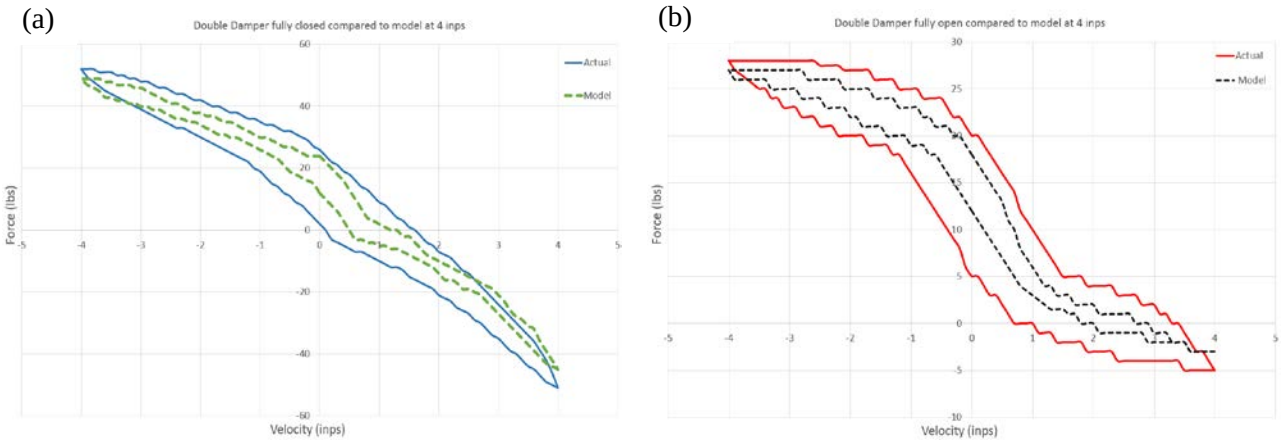

Figure 48: *Double damper Force v/s velocity correlation at 4 in/sec for (a) Fully closed valve (b) Fully open valve*

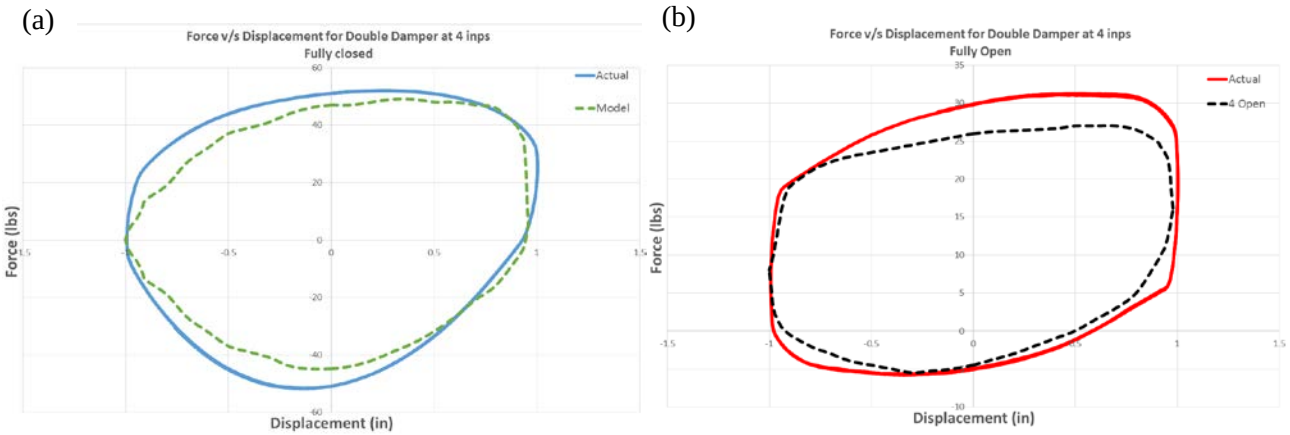

Figure 49: *Double damper Force v/s displacement correlation at 4 in/sec for (a) Fully closed valve (b) Fully open valve*

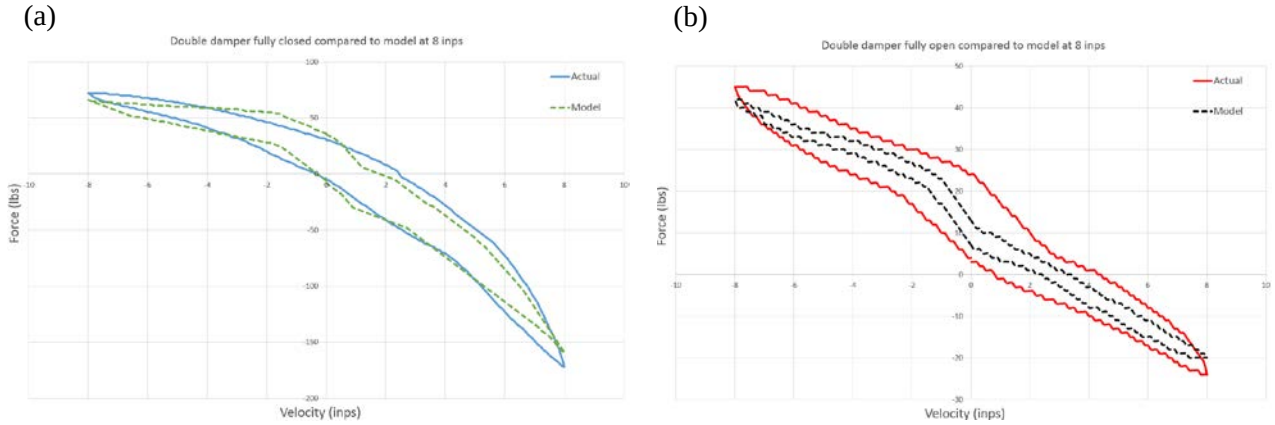

Figure 50: *Double damper Force v/s velocity correlation at 8 in/sec for (a) Fully closed valve (b) Fully open valve*

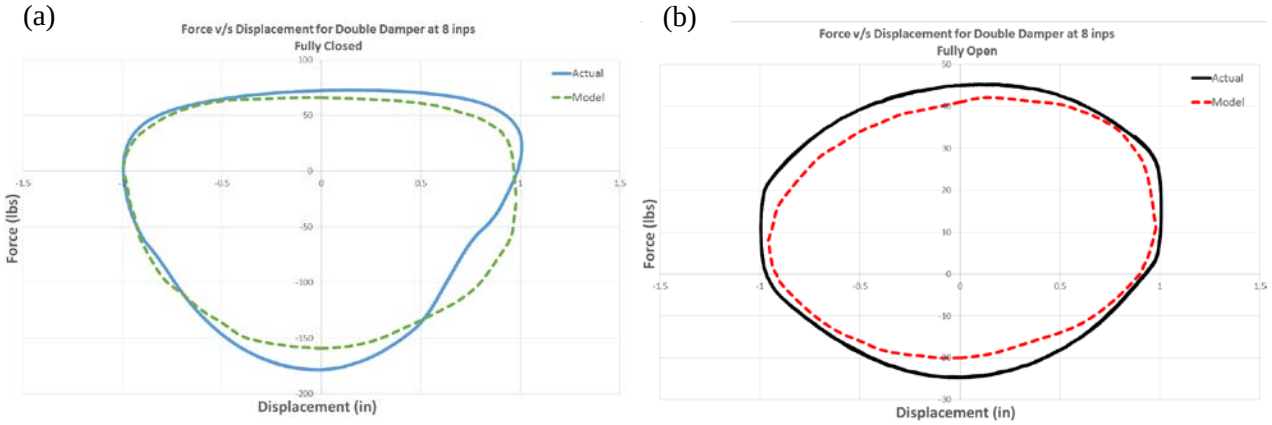

Figure 51: *Double damper Force v/s displacement correlation at 8 in/sec for (a) Fully closed valve (b) Fully open valve*

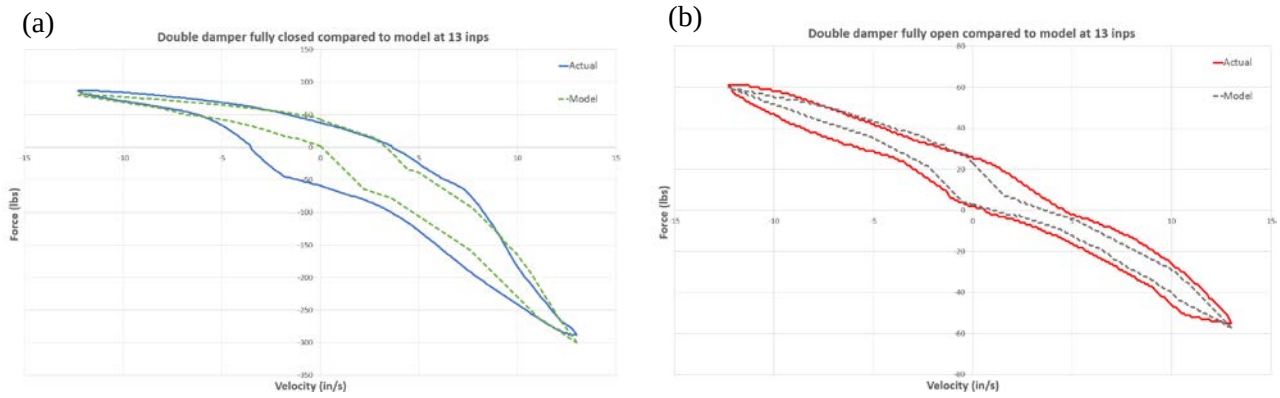

Figure 52: *Double damper model correlation at 13 in/sec for (a) Fully closed valve (b) Fully open valve*

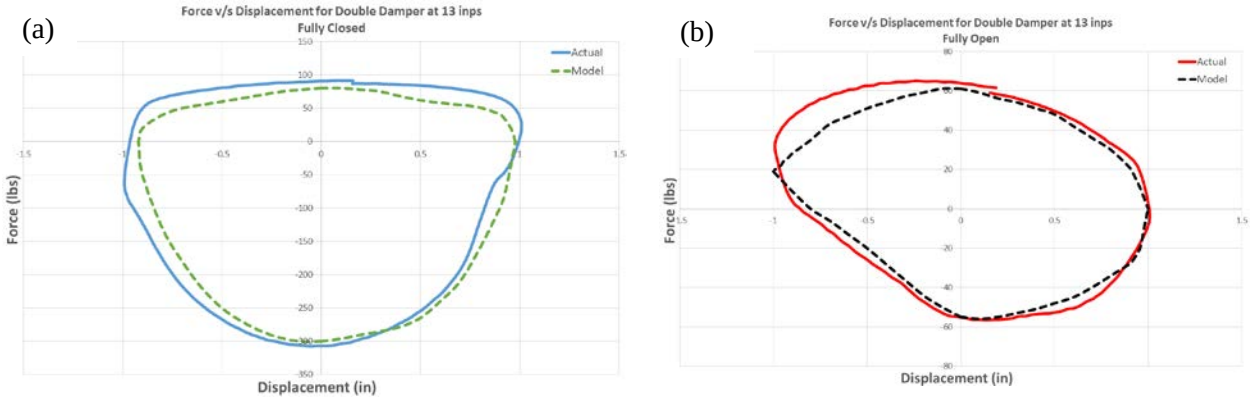

Figure 53: *Double damper Force v/s displacement correlation at 13 in/sec for (a) Fully closed valve (b) Fully open valve*

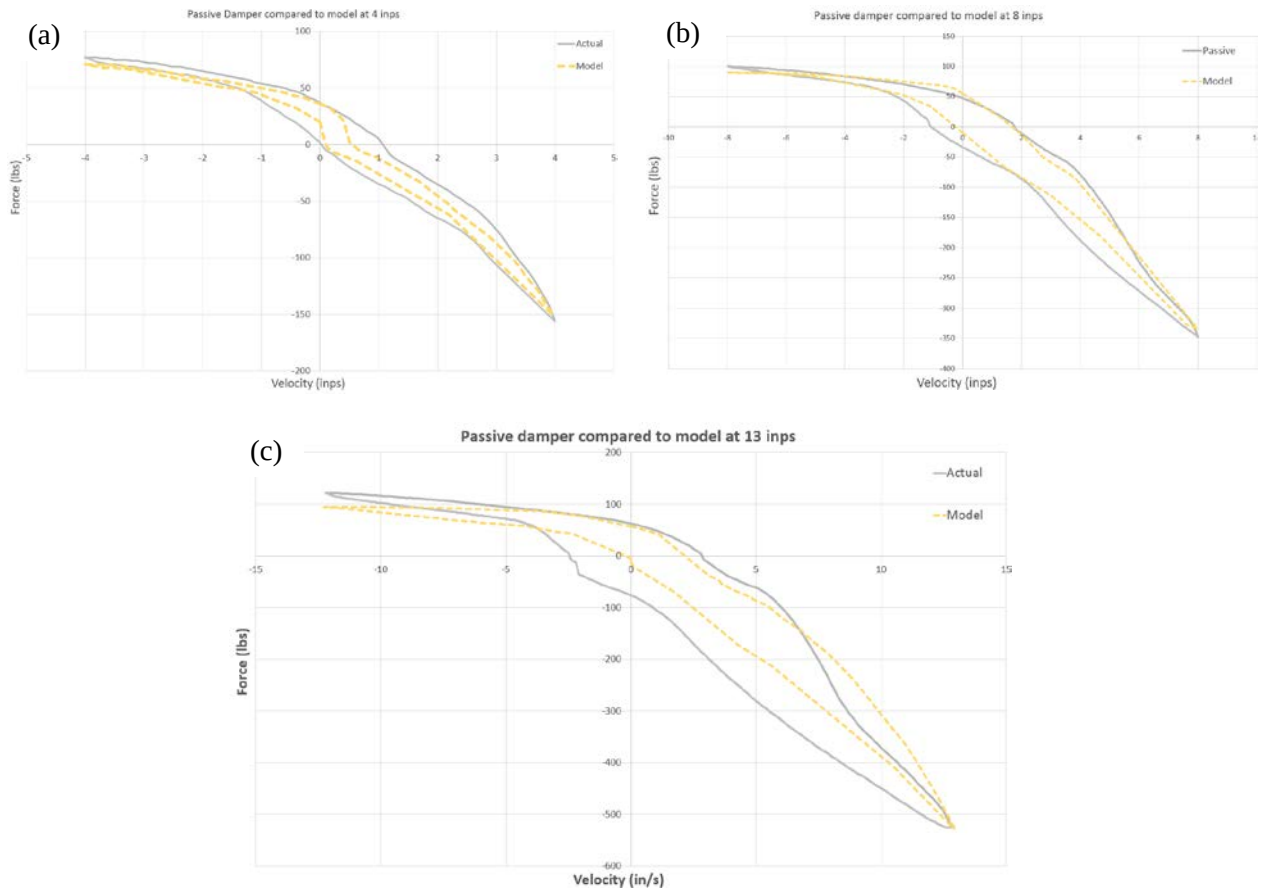

Figure 54: *Model correlation for passive damper (a) 4 in/sec (b) 8 in/sec (c) 13 in/sec*

The results obtained from the model are as shown. The peak forces obtained in compression and rebound are not the same as that of the test results but are still within 10% of the tested value. This is due to a multitude of factors including change in gas pressure, friction force due to bearing and piston, loss in pressure in hoses, shape of semi-active orifice and incorrect modeling of shim stack. The shim stack has currently been modeled as one solid lump of steel with force applied on the bottom face and the hole center being fixed. In reality, multiple shims build the stack and interact with each other. This causes the results of the tail end in each case to be more digressive in nature unlike the Fox damper which is designed to be more

linear in nature. Moreover the shim stack is also constrained on the top with a nut. This creates a discrepancy in the slope of the graph especially at higher speeds where the shim stack plays a larger role. The hysteresis loop observed in each model is also much smaller than the one observed during testing. Since the factors mentioned above are not modeled accurately, there is a significant difference obtained in the final slopes of each graph. The difference observed is much higher at higher speeds and for rebound. Nevertheless the peak forces obtained and the shape of the curve resembles the one obtained in the test data. So correlation of the model does take place. In the future, more accurate modeling of the shim stack and hysteresis loop can be carried out to obtain a more predictable response.

5.4 Peak Forces

Based on the results obtained, the peak forces of all the tests were compiled into one table and are shown below. The passive damper experiences the highest forces as it has lesser controllability. The double damper sees the largest variation in force. The double damper when compared to the passive damper results in a decrease in the total amount of force as the two dampers are in series when the valves are closed and open. The value of the force change as the valve is fully open or fully closed for both dampers. The force variation in the damper is 45 lbs in compression and 220 lbs in rebound at higher speeds and 22 lbs in compression and 45 lbs in rebound at lower speeds.

Table 3: *Peak forces experienced while testing all three dampers*

Velocity (in/sec)	**Stroke**	**Condition of valve (Fully)**	**Peak forces of damper being tested (in lbs)**		
			Single Passive	**Single Semi-active**	**Double**
4	Rebound	Closed	-156	-37	-51
		Open		-20	-5
	Compression	Closed	77	59	42
		Open		52	28
8	Rebound	Closed	-348	-167	-172
		Open		-103	-24
	Compression	Closed	100	78	72
		Open		72	45
13	Rebound	Closed	-526	-260	-288
		Open		-220	-55
	Compression	Closed	121	110	87
		Open		88	61

Chapter 6

Conclusion

A double damper was designed and fabricated. A physics based model of the damper was created to study the flow conditions within the damper. The double damper was then tested against a single semi-active damper and a passive damper of equivalent size. Shock dyno testing was conducted to determine force v/s velocity curves and were then compared to the graphs being obtained by the model.

The double damper for the same size has a much greater range of damping. Using a low power bidirectional valve, it was shown that significant change in damping force could be obtained by adding the valve as a bypass circuit for both dampers. The valves in series can create a much larger difference when compared to an equivalent single semi-active damper. This has great implications in the usage of dampers and allows one to increase the range of available damping which thus leads to a drastic change in performance as shown by the simulation. The increase in available damping along with the implementation of the appropriate controller is what essentially allows the double damper to have superior performance. The design of the damper and the sizing of the various components allows one to decide the range of possible damping and the controller then works in tandem with the sensors to always allow the appropriate amount of area to be selected so as to offer optimum damping in any condition. This can thus be used to tune the ride, handling and comfort of a vehicle by varying each damper according to the need of the moment. The valves in one damper can essentially be completely closed thus using the damper as a solid bar and the other damper can be used to absorb energy. This can be taken one step further where one damper is set up and controlled completely for

performance and the other for comfort, which is essentially what using a Ground-hook-Skyhook control policy allows us to do.

The main objective of this research was to build a quick electrohydraulic prototype and see if the response obtained was any different from that of a single passive shock and whether there would be any unusual spikes or transitions when the upper damper got activated. For that reason, a fairly small sized cheap valve was used and the shim stack was kept the same so as to be able to validate the actual physics of having two dampers in series. Based on these decisions, the range of force obtained is much lower than comparable state of the art semi active dampers. The peak forces were also lower than that of a passive damper as the shim stack used in both dampers was the same as that of the single passive damper. Also, since two fixed orifices were used, the response when the valves are fully open does not match the response of the passive shock. But when the valves are closed, the response of a passive damper can be recreated. So based on varying the flow through each of the four components, varied responses can be obtained without any abnormality. But to be able to produce a production level damper which can compete with the current state of the art in semi-active dampers, it would be advisable to use two MR dampers or to use valves with a much greater range of activation in series so as to be able to get a larger variation in force and also get a more predictable response based on the voltage input into the system.

Future Work and recommendations

- The damper can be tested further on a shock dynamometer to observe changes in damping value based on different shim stacks being used. The damper essentially allows four parameters to vary the damping value: the shim stack in the upper and lower chambers and the controller in the upper and lower chambers. The four variables can be changed to get different levels of damping and thus increase the allowable range even further.

- A more accurate model for the shim stack can allow greater freedom in using the model to vary all the parameters. Currently the results of the model do not accurately tally with the results obtained during testing. More rigorous modeling of the shim stack using energy methods [17] or uniform thickness plates [19] allows more accurate results to be obtained thus eliminating the difference obtained at the tail end of the curves.

- A model to predict the required damping characteristics of a particular vehicle can be created to understand what the preferred curve of the particular application is. Once this is obtained, the double damper model can be used to fine tune the four components and each component can be sized accordingly.

- The valve being used has not been tested for time response under pressurized conditions. A feedback controller can be implemented and the change in orifice area can be observed based on voltage input. Under pressurized conditions the time response should preferably be under 50 milliseconds.

- Quarter-car testing for the damper along with two independent springs needs to be conducted to confirm the results obtained in the simulation. The feedback controller along with the skyhook-ground-hook control policy will be implemented and change in acceleration of the unsprung and sprung mass acceleration can be observed. This is essential to understanding the actual working of the damper in real world conditions.

- Once the damper has proven the concept and validated the simulation, a production version of the damper that is more compact and uses more sophisticated valves can be used. A design for the same has been created and is as shown. This allows a drastic reduction in height and makes the damper compact enough to be used on all sizes of automobiles. The design is essentially a modification of a twin tube design and can be configured to use MR fluid or an internal solenoid. The semi-active mechanism used should preferably have a much greater range of damping.

The final production version of the design consists of an internal damper assembly. The outer tube of the internal damper consists of a piston machined along the exterior wall. As the internal damper experiences force through its lower eyelet, the piston and rod move internally. This allows a certain amount of damping. The resultant damped force then tries to accelerate the internal damper body which forces fluid to flow from the area around the internal damper body through the secondary piston. This sliding of the internal damper body in the external body thus creates an additional damping force. This results in a force acting on the eyelet after having undergone damping through two pistons. This damper essentially resembles a twin tube design in which both tubes are manufactured and assembled independently.

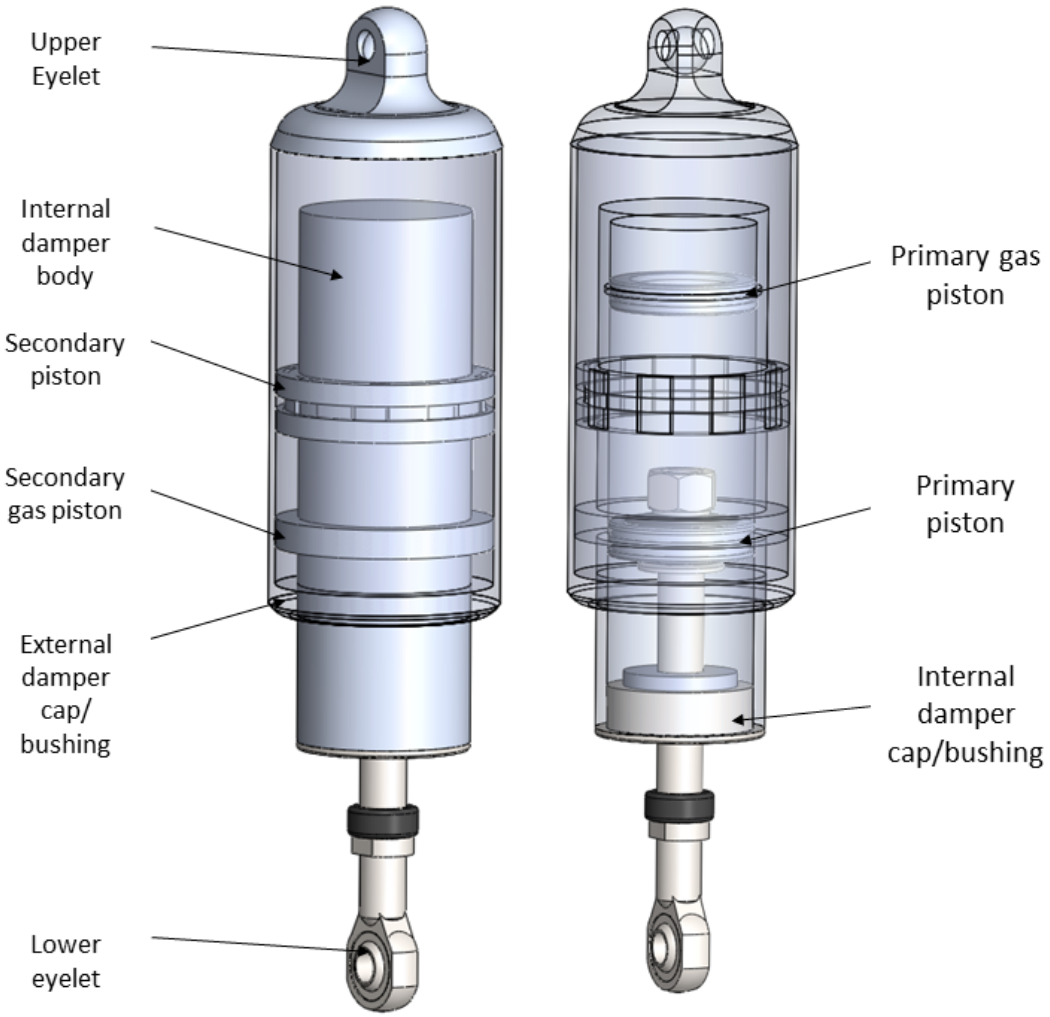

Figure 55: *Production version of double damper*

Bibliography

[1] N. Eslaminasab, "*Development of a Semi-active Intelligent Suspension System for Heavy Vehicles,"* 2008.

[2] B. Ebrahimi and B. Hamesee, "*Development of Hybrid Electromagnetic Dampers for Vehicle Suspension Systems."* 2009

[3] T. Gillespie, "*Development of Semi-active Damper for Heavy Off-road Military Vehicles*." University of Waterloo, 2006.

[4] S.M. Savaresi, C. Poussot-Vassal, C. Spelta, O. Sename, L. Dugard, "*Semi-Active Suspension Control Design for Vehicles*", Elsevier, 2010

[5] D. Karnopp, M. J. Crosby, and R. A. Harwood, "Vibration Control Using Semi-Active Force Generators," *J. Eng. Ind.*, vol. 96, no. 2, pp. 619–626, 1974.

[6] D. Fischer and R. Isermann, "Mechatronic semi-active and active vehicle suspensions," *Control Eng. Pract.*, vol. 12, no. 11, pp. 1353– 1367, 2004.

[7] D. Karnopp, "Design principles for vibration control of systems using semi-active dampers," *Trans. ASME*, vol. 112, p. 448-455, 1990.

[8] D. Karnopp, "Active Damping in Road Vehicle Suspension Systems", *Vehicle System Dynamics, Vol. 12, Iss. 6,* 1983.

[9] Milliken, W., "Active Suspension," *SAE Technical Paper 880799*, 1988.

[10] W. C. T. Burke, "Large Force Range Mechanically Adjustable Dampers for Heavy Vehicle Applications," 2010.

[11] K. J. Kitching, D. J. Cole and D. Cebon, "Performance of a Semi-Active Damper for Heavy Vehicles," *J. Dyn. Sys., Meas., Control* 122(3), 498- 506, 1998.

[12] S-R. Hong, G. Wang, W. Hu, N. M. Wereley, and J. Niemczuk, "An automotive suspension strut using compressible magnetorheological fluids,"

Proc. SPIE - Int. Soc. Opt. Eng., vol. 5760, pp. 238–246, 2005.

[13] G. W. Groves, Karl Kazmirski, "*Solenoid actuated continuously variable shock absrober*." Google Patents, 24-July-2000.

[14] J. D. Carlson and M. J. Chrzan, "Magnetorheological fluid dampers." Google Patents, 11-Jan-1994.

[15] Mehdi Ahmadian, Christopher A. Pare, "A Quarter-Car Experimental Analysis of Alternative Semiactive Control Methods", *Journal of Intelligent Material Systems and Structures,* 2000.

[16] Shulman, Z. P., V. I. Kordonsky, E. A. Zaltsgendler, I. V. Prokhorov, B. M. Khusid, and S. A. Demchuk, "Structure, Physical Properties and Dynamics of Magnetorheological Suspensions" *International Journal of Multiphase Flow,* 1986. 12(6): p. 935-955.

[17] Alireza Farjoud, "*Physics-based Modeling Techniques for Analysis and Design of Advanced Suspension Systems with Experimental Validation*", 2011.

[18] John Dixon, "T*he Shock Absorber Handbook, 2nd Edition*". Wiley, 2007.

[19] M. S. Talbott and J. Starkey, "An Experimentally Validated Physical Model of a High-Performance Mono-Tube Damper," *SAE Tech. Pap Ser.*, no. 724, 2002.

[20] K. S. Rhoades, "Development and experimental verification of a parametric model of an automotive damper", 2006.

[21] Reybrouck K.G., "A Non Linear Parametric Model of an Automotive Shock Absorber*", SAE Technical Paper Series 940869*, 1994.

[22] P. T. Wolfe, C. M. Nobles, and L. R. Miller, "*Semi-active damper piston valve assembly*." Google Patents, 1989.

[23] P. T. Wolfe, "*Improved valving for a controllable shock absorber.*"

Google Patents, 02-June-1993.

[24] K. Reybrouck, "*Damper with externally mounted semi-active system*", Google Patents, 27-Nov-2001

[25] G. Vanhees, K. Reybrouck, "*Shock absorber having a continuously variable semi-active valve.*" Google Patents, 29-Jun-2010.

[26] Randal L. Derr, "*Low level damping valve and method for a semi-active hydraulic damper*", Google Patents, 17-Nov-1992

[27] Y. Siramdasu, "A New Semi-Active Suspension System for Vehicle Applications," *Int. J. Mod. Eng.*, p. 8, 2013.

[28] D. A. Palmer, "*Piston valve assembly for a shock absorber*", Google Patents, 01-Sept-1977.

[29] Lang H.H., "*A Study of the Characteristics of Automotive Hydraulic Dampers at High Stroking Frequencies"*, 1997.